The Influence of Metal Substrates on the Electronic States of Metal Overlayers

P. A. Dowben
Syracuse University

M. Onellion
University of Wisconsin

Y. J. Kime
Syracuse University

Follow this and additional works at: https://digitalcommons.usu.edu/microscopy

Part of the Biology Commons

Recommended Citation

Utah State University
MERRILL-CAZIER LIBRARY

THE INFLUENCE OF METAL SUBSTRATES ON THE ELECTRONIC STATES OF METAL OVERLAYERS

P. A. Dowben*[1], M. Onellion**, and Y. J. Kime*

*Department of Physics, Syracuse University, Syracuse, New York, 13244-1130
**Department of Physics, University of Wisconsin, Madison, Wisconsin, 53706

Abstract

The aim of this paper is to provide an introduction to the electronic structure of very thin film (one to ten monolayers) overlayers using examples from studies of Hg overlayers on Ag(100) and Fe thin film overlayers. Interfacial states as a result of the interaction of the substrate and overlayer, as well as the new electronic states of the overlayer caused by a new crystallographic structure can modify the overlayer metal electronic structure. Additional changes in the overlayer electronic stucture arise from the reduced dimensionality (2 dimensionality as opposed to 3 dimensionality) of the thin film. We discuss the photoemission techniques for determining the electronic structures of thin metal overlayers. Layer by layer growth of the overlayer is important for such studies as is knowledge of the overlayer structure. We have summarized our current understanding of metal overlayers in tables and attempt to demonstrate that further progress in combining structural and photoemission studies is necessary for better fundamental understanding of metal overlayers.

[1]Address for correspondence:
P. A. Dowben
Dept. of Physics, Syracuse University
Syracuse, New York 13244-1130
                    Phone No. (315)423-2408

Introduction

Metal overlayers have been investigated since the late 1800's for use in a variety of applications, e.g.,for incandescent light bulbs. Within the last several years researchers have begun investigating very thin metal overlayers, one to ten monolayers thick. Several reviews [1-9] exist describing various aspects of this effort, to which the reader is referred. The present review focuses on the influence of the metal substrate, in particular the influence of the substrate on the thin film overlayer electronic structure. We concentrate on two particular metal overlayer systems: Hg on Ag(100) and Fe overlayers on different substrates. Following a brief discussion of overlayer film growth and of angle resolved photoemission, the Hg on Ag(100) results are used to illustrate several key results that may be generalized for many overlayer systems. Since one of the most exciting frontiers of metal overlayers is in the area of magnetic systems, a concise summary of this aspect of electronic structure is presented, with iron overlayers used to exemplify the most important features of the endeavour.

Often epitaxial crystal structures can be grown on convenient substrates, in a well controlled and well characterized manner. The resulting overlayer thin film may have unusual lattice spacings and/or crystal structure. The opportunity to create new materials is one advantage that metal-metal heterostructures have over other bimetallic (or indeed any multi-component metal) systems such as alloys. Alloys are difficult to characterise and alloy surfaces, in particular the surfaces of weakly clustering alloys (as opposed to strongly ordered alloys), are very difficult to characterise, while the selvedge (surface region) of all alloys remains largely uncharacterised [10-12]. Thin film metal overlayers, by comparison, are relatively easy to characterise structurally.

Metal Overlayer Film Growth

In studying the effects of various substrates on metal overlayers, Frank-van der Merwe (layer by layer) growth is desired so as to easily model the substrate/overlayer system. For one to ten monolayer overlayer films, confirming

the growth mode in itself is a formidable problem. Most commonly, overlayer growth is investigated using low energy electron diffraction (LEED) [13-86] and less commonly reflection high energy electron diffraction (RHEED) [58,87-104]. Techniques that have also been used to characterize thin film growth include transmission electron microscopy and diffraction methods applied to thin films detached from their substrates or at grazing incidence to the thin film and substrate [7,105-114]. Overlayer thin films can be characterized for thin films grown in situ in the ultra high vacuum (UHV) micro-scope [75,115-121] or by using surface extended X-ray absorption fine structure (SEXAFS) [24,122]. In addition, forward scatter-ing [123-136] in X-ray photoemission (XPS) and Auger electron spectroscopy (AES) may provide a new method for acquiring additional information on the structure of thin film overlayers.

Different types of increases in the AES and XPS elemental signals with overlayer deposition can also be used to supplement LEED and RHEED and can prove to be a good indication of layer by layer growth as described elsewhere [7]. Not only do the changes in characteristic elemental signals as the thin film grows from one layer to the next become indicative of layer by layer growth, but the simple scattering of AES electrons by defects [137] can cause line shape changes. This results in periodic AES signal oscillations resulting from the waxing and waning of the step densities with layer by layer growth [106,138-140]. The core level binding energies can also be of considerable assistance in characterising the thin film metal over-layer [17,37,62,141-148] either from inspection of the binding energy shift or from application of a Born-Haber cycle through the use of an "equivalent cores approximation" (Reference 148 and the references therein).

Due to the difficulties of achieving conclusive structural information, many studies of the overlayer thin film electronic properties to date have only inferred the film structure and morphology. This is widely recognized as an unfortunate situation, and several research groups will shortly have the capabilities to investigate both electronic and structural properties. Studies of the electronic structure of metal on metal overlayers are very suspect when undertaken without careful analysis of the overlayer structure and growth mode. LEED patterns alone, such as those shown in Figure 1 for Hg overlayers of Ag(100), are insufficient indication of the growth mode and the micro-structure of the surface.

When layer by layer growth occurs [5-7,149-157] there is epitaxial or pseudomorphic growth only up to some critical thickness h_c as a result of the lattice misfit strain. For overlayer growth beyond the critical metal film thickness h_c, interfacial dislocations become incorporated in the film during the growth process. This results in a decrease in the lattice misfit strain as the metal overlayer becomes thicker. This situation is applicable
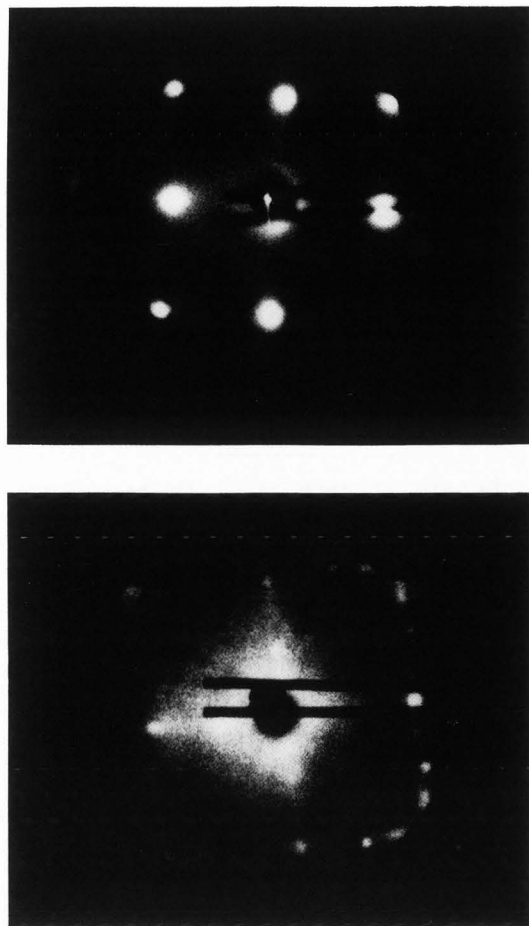
Figure 1. LEED patterns of Hg overlayers of Ag(100). The top pattern shows the p(1x1) structure (identical to the substrate) that occurs following an exposure of 6 langmuirs $(6 \times 10^{-6}$ torr seconds) of Hg to Ag(100) at 87 K. This corresponds to the deposition of two mono-layers of Hg on Ag(100). The bottom LEED pattern shows the p(1x4) overlayer formed by depositing five monolayers of Hg on Ag(100) at 87 K (15 langmuirs exposure).

only to small lattice misfits f_o. For cubic crystals, f_o is defined as:

$$f_o = (a_s - a_f)/a_s \qquad (1)$$

where a_s and a_f are the bulk lattice parameters of the substrate and overlayer metals, respectively. When large misfits are present, the continuation of the substrate lattice does not occur in the metal overlayer (no pseudo-morphism). Interfacial dislocations are immediately present after growth begins if f_o is much larger or smaller than zero. With inter-facial dislocations present at all stages of growth for the thin film overlayer, the inter-

facial strain decreases as 1/h, where h is the overlayer thickness. Assuming there is no alloying, interdiffusion or other changes at the interface, Frank-van der Merwe growth [5,150-153] implies that:

$$\Delta\epsilon = \sigma_f + \sigma_i - \sigma_s \leq 0 \text{ and} \qquad (2)$$

$$\sigma_s \geq \sigma_f + \sigma_i \qquad (3)$$

where σ_f and σ_s are the specific free energies of the film and substrate, respectively, while σ_i is the specific free interfacial energy. Markov and Kaischew [155-156] have modified equations 2 and 3 but some of their conclusions about the conditions for layer by layer growth have been questioned by Bauer and van der Merwe [157].

In practice, for pseudomorphic growth in the Frank-van der Merwe growth mode, the lattice mismatch should be less than 9% [149]. This does not mean, of course, that with large lattice mismatches ordered monolayer thin films cannot be deposited on a crystalline substrate, only that the ordered structure of the overlayer is not identical to that of the substrate. Such ordered overlayers are commonly observed as indicated in Table 1.

Often it is very difficult to distinguish between the initial stages of Frank-van der Merwe growth modes and Stranski-Krastanov growth (growth of three dimensional islands and crystals on a thin metal film that initially grew layer by layer). Initial layer by layer growth does not imply this growth mode continues to all thicknesses. Furthermore, interdiffusion may sometimes be confused with layer by layer growth [29].

Angle-Resolved Photoemission

Angle-resolved photoemission is the dominant technique for determining an overlayer electronic band structure. The photoemission process consists of the absorption of one photon and the subsequent ejection and detection of the photoelectron from the photoionized atom. Because the photoemission final state includes an ion (an excited state), several complexities arise including screening, final state effects and many body effects. In most examples of photoemission the simple picture just described is valid.

The intensity (or counts) of the detected photoelectrons, at a given photon energy, is plotted against electron kinetic energy for a given photon energy. This energy distribution curve (EDC) provides a rough picture of the density of states for a particular photon incidence angle and electron emission angle. Neglecting the complexities of the photoemission process, in general, the kinetic energy of the photoelectron is given by:

$$E_{kin} = h\nu - \phi - E_B \qquad (4)$$

where $h\nu$ is the photon energy, ϕ is the work function, and E_B is the binding energy of the electron relative to the Fermi energy.

Highly polarized light can be useful in determining the orientation and symmetry of an electronic state by using dipole selection and symmetry rules [158-162]. By varying the incidence angle of the light θ_i and the orientation of the vector potential $\underline{A}$ with respect to the surface crystal lattice (azimuthal orientation) as well as the emission angle of the photoelectron θ_e (as indicated in Figure 2), one can often elucidate the symmetry of a particular state. For example, the character of orbitals excited for two different orientations of the electric vector $\underline{E}$ (or vector potential $\underline{A}$) with respect to the surface normal is indicated in Table 2 for a four fold (C_{4v}) symmetric surface (e.g., the (100) plane of an f.c.c. or b.c.c. crystal). The symmetry of the initial state of the electron, as summarized in Table 3, must be the same as that of the dipole operator (the perturbed Hamiltonian) that causes the transition (photoemission). It is clear that incidence and emission angular resolution results in selection [161,163] of the initial and final state symmetries as shown in Table 3. Not only must the initial state be of the same symmetry as the dipole operator but the final state as well. Photoemission may be regarded as an interband transition from a bound state to a free electron state for which:

$$E_{kin} = p^2/(2m) = k^2h^2/(8\pi^2m) \qquad (5)$$

The experimental band structure is mapped out by collecting electrons at different emission angles and points in k-space (where $\underline{k}$ is the wave number of the photoelectron). The binding energies of the photoemission features are plotted as a function of $\underline{k}$. The free electron bands are generally regarded as parabolic (on an
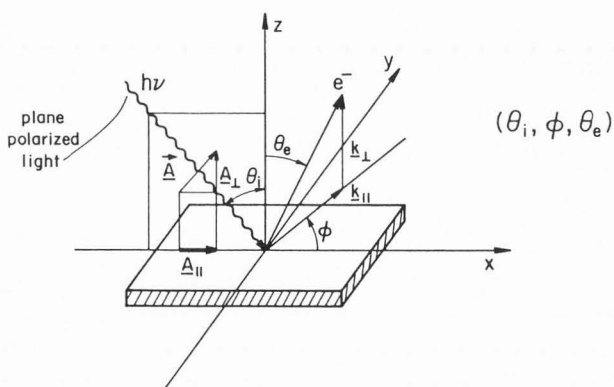
Figure 2. The geometry of angle resolved photoemission indicating incidence angle θ_i, electron emission angle θ_e, and orientation angle of the electron wave vector with respect to the crystal ϕ. As is indicated in the figure the vector potential of the incident light has a perpendicular component and parallel component with respect to the surface as does the electron wave vector.

Table One

Metal/metal:	coverage:	exchange splitting:	overlayer structure:	lattice change:	interface states:	new states:	growth mode:	Work function changes:
Ag/Cu(100)	1 ml	–	c(10x2)[13,14]	-1.7%	no[13,14]	–	–	–
Ag/Cu(111)	1-10 ml	–	–	–	yes[258]	–	FvdM[258] SK[106]	–
Ag/Pt(100)	1-2 ml	–	–	–	yes[17]	–	–	–
Ag/Pt(997)	1-2 ml	–	–	–	yes[17]	–	–	–
Ag/Rh(100)	–	–	–	–	–	–	FvdM[259]	–
Ag/W(211)	1 ml	–	p(1x1)[15]	-5.1%	–	–	–	-0.4[15]
Au/Ag(111)	1-4 ml	–	p(1x1)[16]	-1.8%	yes[258,260]	–	FvdM[261]	–
Au/Pt(100)	1-2 ml	–	p(1x1)[17]	+5.0%	yes[17]	–	–	-0.45[17]
Au/Pt(111)	1-2 ml	–	–	–	yes[17]	–	–	-0.3[17]
Au/Pt(997)	1-2 ml	–	–	–	yes[17]	yes[17]	–	–
Au/Ru(0001)	1-3 ml	–	p(1x1)[18]	-8.1%	–	–	FvdM[18]	–
Au/W(100)	1 ml	–	p(2x1)[19-21]	–	yes[19]	–	–	+0.5[19-22]
Au/W(110)	1 ml	–	p(1x1)[21]	-5.2%	–	–	–	+0.5[21]
Au/W(211)	1 ml	–	p(1x1)[15,21]	-5.2%	–	–	–	+0.5[15,21]
Bi/Cu(100)	1-3 ml	–	complex[25]	+2.9%	–	–	–	–
Co/Cu(100)	1-3 ml	1.0 ev[23]	p(1x1)[23] c(2x2)[23]	-2.0%	yes[23]	–	FvdM[23]	–
Co/Cu(111)	1 ml	0.7 ev[221,222]	p(1x1)[23-24,122]	-2.0%	–	–	FvdM[23-24,122]	–
Co/Cu(111)	2 ml	0.7 ev[221]	p(1x1)[23-24,122]	-2.0%	–	–	FvdM[23-24,122]	–
Co/GaAs(110)	100 ml	–	p(1x1)[89]	-2.4%	–	–	–	–
Cr/Au(100)	1-15 ml	–	(1x1)[26]	0%	yes[26]	yes[26]	SK[26]	–
Cu/Ag(100)	1 ml	–	p(1x1)[27,28]	+13%	yes[27]	–	FvdM[27]	–
Cu/Al(111)	1 ml	–	interdiffusion[29]	–	–	–	–	–
Cu/Nb(110)	1 ml	–	complex[30]	-8.8%	–	yes[30]	–	–
Cu/Nb(110)	2 ml	–	complex[30]	-0.5%	–	–	–	–
Cu/Ni(100)	1 ml	–	p(1x1)[31-33]	+2.6%	–	–	–	–
Cu/Ni(100)	100 ml	–	p(1x1)[107]	+2.6%	–	–	–	–
Cu/Pd(100)	1-2 ml	–	p(1x1)[34-35]	+7.6%	yes[34]	yes[34]	FvdM[34,35]	-0.8[34]
Cu/Pd(100)	>2 ml	–	–	–	yes[34]	yes[34]	SK[34]	–
Cu/Pt(111)	1-10 ml	–	p(1x1)[36,85]	+7.4%	yes[36,37]	yes[36]	FvdM[36]	-1.26[36]
Cu/Ru(0001)	1 ml	–	p(1x1)[38]	+3.7%	yes[38]	yes[38]	FvdM[38]	–
Cu/Ru(0001)	>1 ml	–	–	–	–	–	SK[251]	–
Fe/Ag(100)	1 ml	none[40]	p(1x1)[39-40]	+11%to-0.8%	yes[40]	–	FvdM[39]	+0.9[39]
Fe/Ag(100)	2-3 ml	none[40]	p(1x1)[39-40]	+11%to-0.8%	yes[40]	–	FvdM[39]	+0.5[39]
Fe/Ag(100)	>3 ml	0.3 ev[40]	p(1x1)[40]	+11%to-0.8%	–	–	SK[39]	–
Fe/Cu(100)	1 ml	2.65 eV[41]	p(1x1)[41-45]	+3.1%	yes[41]	yes[41]	FvdM[42-44]	–
Fe/Cu(100)	2 ml	2.65 eV[41]	p(1x1)[41-45]	+3.1%	yes[41]	yes[41]	FvdM[42-44]	–
Fe/Cu(100)	1-17 ml	none[199]	p(1x1)[41-44]	+3.1%	none[199]	yes[199]	FvdM[42-44]	–
Fe/GaAs(110)	>10 ml	2.0 ev[112]	p(1x1)[112]	-1.38%	–	–	–	–
Fe/V(poly)	–	–	–	–	yes[114]	yes[114]	–	–
Fe/W(110)	1 ml	(0.6 eV)[46]	p(1x1)[46-47]	+10.5%	yes[46]	yes[46]	FvdM[46-47]	–
Fe/W(110)	2 ml	(0.5 eV)[46]	p(1x1)[46-47]	+10.5%	yes[46]	yes[46]	FvdM[46-47]	–
Fe/W(110)	3-10 ml	(0.3 eV)[46]	p(1x1)[46-47]	+10.5%	–	no[46]	FvdM[46-47]	–
Hg/Ag(100)	1 ml	–	p(1x1)[48-49]	-3.8%	yes[48-49]	yes[48-49]	FvdM[48-49]	-0.16[252]
Hg/Ag(100)	2 ml	–	p(1x1)[48-49]	-3.8%	yes[48]	yes[48-49]	FvdM[48-49]	–
Hg/Ag(100)	5 ml	–	p(4x1)[48]	-3.8%	–	yes[48]	FvdM[48-49]	–
Hg/Au(poly)	<1 ml	–	–	–	none[215]	no[215]	–	-0.2[252] -0.45[253,254]
Hg/Cu(100)	1 ml	–	c(2x2)	+20.2%	none	no	FvdM	–
Hg/Fe(100)	1 ml	–	p(1x1)[51]	-4.6%	–	–	FvdM[51]	–
Hg/Ni(100)	1 ml	–	c(2x2)[50]	+17.1%	none[214]	no[214]	FvdM[50]	–
Hg/W(100)	1 ml	–	p(1x1)[52]	+5.2%	yes[216,217]	yes[216]	FvdM[52,53]	+.3[255]
Ni/Al(poly)	<5 ml	none[220]	–	–	–	–	–	–
Ni/Cu(100)	1-2 ml	0.3 eV[227]	p(1x1)[54]	-2.6%	–	–	FvdM[54]	–

Table One continued

Metal/metal:	coverage:	exchange splitting:	overlayer structure:	lattice change:	interface states:	new states:	growth mode:	Work function changes:
Ni/Cu(100)	>3 ml	–	p(1x1)[54,107]	-2.6%	–	–	SK[54]	–
Ni/Cu(111)	<5 ml	–	p(1x1)[55-56,85-86]	-2.6%	–	–	FvdM[55-56,87-88]	–
Ni/In(poly)	<2.5 ml	none[226]	–	–	–	–	–	–
Ni/Mg(poly)	<2.5 ml	none[226]	–	–	–	–	–	–
Ni/Pb$_3$Bi	<2 ml	none[224]	–	–	–	–	–	–
Ni/Re(0001)	<2.5 ml	none[230]	p(1x1)[230]	+10%	–	–	–	–
Ni/Sn(poly)	<2.5 ml	none[226]	–	–	–	–	–	–
Ni/W(110)	<1 ml	–	p(1x1)[57]	+9.1%	–	–	SK[57]	-0.76[57]
Ni/W(211)	<1 ml	–	p(1x1)[57]	+9.1%	–	–	SK[57]	-0.6[57]
Pb/Ag(111)	1-3 ml	–	($\sqrt{3}$x$\sqrt{3}$)[58-59,75]	-0.6%	–	–	FvdM[58]	–
Pb/Ag(111)	>3 ml	–	complex[58,75]	0%	–	–	FvdM[58]	–
Pb/Al(100)	1-2 ml	–	c(2x2)[60]	+15.7%	–	–	FvdM[60]	–
Pb/Al(111)	1 ml	–	–	–	–	–	SK[62]	-0.1[62]
Pb/Cu(100)	1 ml	–	c(2x2)[61,63]	+3.3%	–	–	SK[61]	–
			c(5x1)[25,64]	+0.5%				
Pb/Cu(110)	1 ml	–	p(5x1)[63,64,113]	-8.9%	–	–	–	–
Pb/Cu(111)	1 ml	–	p(4x4)[64,65]	-2.9%	–	–	FvdM[65] Sk[58]	–
Pb/Ni(111)	–	–	–	–	–	–	–	-0.7[62]
Pb/Pt(111)	1 ml	–	(3x3)[66]	–	–	–	–	–
Pb/W(100)	1 ml	–	p(1x1)[67]	-9.6%	–	–	SK[67]	+0.1[67]
Pb/W(110)	1 ml	–	p(3x1)[67]	-9.7%	–	–	FvdM[67]	-0.4[67]
Pb/W(110)	2 ml	–	–	–	–	–	SK[67]	-0.7[67]
Pd/Ag(100)	1-3 ml	–	p(1x1)[68]	+5%	yes[68]	–	FvdM[68]	–
Pd/Ag(111)	1-3 ml	–	p(1x1)[68]	+5%	yes[68]	–	FvdM[68]	–
Pd/Au(111)	1-7 ml	–	p(1x1)[69]	+4.8%	yes[69]	yes[69]	FvdM[69]	–
Pd/Cu(111)	1-3 ml	–	p(1x1)[70]	-7.1%	no[70]	no[70]	–	+0.6[70]
Pd/Nb(110)	1 ml	–	p(1x1)[71]	+3.9%	–	yes[71]	–	–
Pd/W(100)	1 ml	–	complex[72]	+2.2%	–	–	FvdM[72]	+0.3[72]
Pd/W(100)	>1 ml	–	complex[72]	+2.2%	–	–	SK[72]	–
Sn/Al(100)	1-2 ml	–	c(2x2)[60]	+45%to35%	–	–	FvdM[60]	–
Sn/Al(111)	1 ml	–	(2x2)[62]	–	–	–	SK[62]	+0.1[62]
Sn/Ni(111)	1 ml	–	($\sqrt{2}$x$\sqrt{3}$)[62]	+95to109%	–	yes[62]	FvdM[62]	-0.5[62]
Sn/Ni(111)	2 ml	–	(2x2)[62]	–	–	yes[62]	FvdM[62]	–
Tl/Ag(111)	1-3 ml	–	($\sqrt{3}$x$\sqrt{3}$)[58]	1.9%	–	–	FvdM[58]	–
Tl/Ag(111)	>10 ml	–	complex[58]	0%	–	–	FvdM[58]	–
Tl/Cu(111)	1 ml	–	($\sqrt{3}$x$\sqrt{3}$)[58]	0%	–	–	SK[58]	–
Tl/Cu(111)	2-10 ml	–	complex[58]	-2.3%	–	–	SK[58]	–
Tl/Cu(111)	>10 ml	–	complex[58]	0%	–	–	SK[58]	–

Table 1. A compilation of data for selected metal overlayers on metal substrates. The orientation of the substrate is indicated by a Miller index. The coverage of the overlayer is provided in monolayers (where known), as is the coincidence lattice, with respect to the substrate. Lattice change indicates the percent expansion or compression of the overlayer adatoms with respect to the nearest neighbor spacings of the bulk metal. The exchange splitting is the splitting of the minority and majority spin states of the magnetic overlayer, and in some cases has been estimated from the splitting of the d-band observed in photoemission and thus may not be an accurate assessment of the exchange splitting. Growth modes of the overlayer are denoted by FvdM for layer by layer growth while layer by layer growth followed by island formation is indicated by SK. The work function change is positive if increasing and negative if decreasing. Both the exchange splitting and work function change are provided in units of eV.

energy versus wave vector plot). The wave vector k (or p/h) of the electron is generally resolved into two components: a component parallel to the surface k_{par} and a component normal to the surface k_{perp} such that:

$$k^2 = k_{par}^2 + k_{perp}^2 \qquad (6)$$

The component of the wave vector of the electron parallel to the surface k_{par} is given by:

$$k_{par} = \left\{ (8\pi^2 m/h^2)E_{kin} \right\}^{1/2} \sin\theta \qquad (7)$$

where θ is the emission angle and E_{kin} is the kinetic energy of the electron. Because of the

Table Two   Dipole Selection Rules for Photoemission for Normal Emission ($\bar{\Gamma}$) and the High Symmetry Lines of a Square Brillouin Zone (SBZ)

component of the vector potential $\underline{A}$	(C_{4v}) $\bar{\Gamma}$	$\bar{\Sigma}$ (C_{1h})	$\bar{\Lambda}$ (C_{1h})
$\underline{A}$ perpendicular to the surface	s p_z $d_{3z^2-r^2}$ (Δ_1)	s p_z p_{x+y} $d_{3z^2-r^2}$ d_{xy} d_{xz+yz}	s p_z p_x $d_{3z^2-r^2}$ $d_{x^2-y^2}$ d_{xz}
$\underline{A}$ parallel with the surface in the electron detection plane (even geometry)	p_x p_y d_{xz} d_{yz} (Δ_5)	s p_z p_{x+y} $d_{3z^2-r^2}$ d_{xy} d_{xz+yz}	s p_z p_x $d_{3z^2-r^2}$ $d_{x^2-r^2}$ d_{xz}
$\underline{A}$ parallel with the surface and perpendicular to the electron detection plane (odd geometry)	p_x p_y d_{xz} d_{yz} (Δ_5)	p_{x-y} d_{xz-yz} $d_{x^2-y^2}$	p_y d_{yz} d_{xy}

The relationship between the orientation of the vector potential of the incident light, the photoelectron collection geometry and the states observed in angle resolved photoemission. Note that the symmetry points are given for the surface Brillouin zone of a four fold symmetric surface such as a (100) face of a b.c.c. or f.c.c. crystal. The nomenclature of the symmetry points and lines are indicated in Figure 3.

relationship between $\underline{k}_{par}$ and $\underline{k}_{perp}$, both surface and bulk band structures can be mapped out using angle resolved photoemission.

Since the parallel momentum of the photoelectron is conserved, the location of the initial state in the surface Brillouin zone can be deduced unambiguously. To determine a location in the bulk Brillouin zone, the effective potential of the atom (the inner potential) must be inferred. In other words, when the photoelectron crosses the interface between the solid and vacuum, k_{par} is conserved but k_{perp} is changed. Thus while k_{perp} may be conserved within a three dimensional crystal, it is not conserved in the photoemission process, and equation 4 must be modified to include a term for the inner potential.

Investigators use the k_{par} conservation to distinguish between overlayer and substrate electronic states (though layer compounds fall into a special category having effectively only two dimensional band structures [164-167]). For a very thin (1-2 monolayer) film an overlayer

electronic state cannot disperse with $\underline{k}_{perp}$. The overlayer state will disperse symmetrically about the high symmetry points of the surface Brillouin zone. Figure 2 illustrates how the surface and bulk band structures are mapped out along the high symmetry lines illustrated in Figure 3. The bands are typically denoted by their group representations (as indicated in Table 3).

A further complication for the unwary experimentalist is diffraction effects. The crystal lattice furnishes momentum in quantities of the reciprocal lattice vector $\underline{G}$. Photoemission processes of crystals not only result in optical band transitions but also Umklapp processes as a consequence of diffraction against the crystal lattice through a reciprocal lattice vector $\underline{G}$. Umklapp processes [168-170] and diffraction effects [171-172] can often lead to confusion and difficulty in mapping out the band structure. In particular, diffraction effects can superficially obscure the band structure. For Ni(100), diffraction effects [171] lead to EDC's at particular photon energies that do not

Table 3. Character Tables and Group Representations for States at High Symmetry Points and Lines of a C_{4v} Surface.

$\overline{\Gamma}$ $\quad$ $\overline{M}$ $\quad$ (C_{4v})

	E	$2C_4$	C_2	$2\sigma_v$	$2\sigma_d$	$\overline{\Gamma}$ top & center$\quad$ $\overline{M}$ top	$\overline{M}$ ctr $\quad$ $(A_1 \leftrightarrow B_2)$ $(A_2 \leftrightarrow B_1)$
A_1	1	1	1	1	1	$1,z,\quad 3z^2-r^2$	xy
A_2	1	1	-1	-1	-1		x^2-y^2
B_1	1	-1	1	1	-1	x^2-y^2	
B_2	1	-1	1	-1	1	xy	1 $\quad$ z $\quad$ $3z^2-r^2$
E	2	0	-2	0	0	$(x,y),\ (xz,yz)$	$(y,x)\quad (yz,xz)$

$\overline{X}$ $\quad$ (C_{2v})

	E	C_2	$\sigma_v(xy)$	$\sigma_v'(yz)$	top	center $\quad (A_1 \leftrightarrow B_1)$ $(A_2 \leftrightarrow B_2)$
A_1	1	1	1	1	$1,\ z,\ 3z^2-r^2, x^2-y^2$	$x \quad xz$
A_2	1	1	-1	-1	zy	$y \quad yz$
B_1	1	-1	1	-1	$x,\ xz$	1 $\ $ z $\ $ $3z^2-r^2,\ \ x^2-y$
B_2	1	-1	-1	1	$y,\ yz$	xy

$\overline{\Sigma}$ $\quad$ (C_{1h})

	E	$\sigma_h(x,y=0)$	top, center
A'	1	1	$1,z,\ (x+y),\ 3z^2-r^2,\ xy,\ (x+y)z$
A''	1	-1	$(x-y),\ x^2-y^2,\ (x-y)z$

$\overline{\Delta}$ $\quad$ (C_{1h})

	E	$\sigma_h(y=0)$	top, center	center
A'	1	1	$1,\ z,x,3z^2-r^2,x^2-y^2,xz$	$1,z,x,3z^2-r^2,x^2-y^2,xz$
A''	1	-1	$y,\quad xy,\quad yz$	$y,\quad xy,\quad yz$

$\overline{Z}$ $\quad$ (C_{1h})

	E	$\sigma_h(x=0)$	top	center
A'	1	1	$1,z,y,3z^2-r^2,x^2-y^2,yz$	x,yz,xz
A''	1	-1	$x\quad xy\quad xz$	$1,z,y,3z^2-r^2,x^2-y^2,yz$

Table 3. The group representations and character tables for the high symmetry points and lines for the surface Brillouin zone of a four fold (C_{4v} symmetric surface). The nomenclature for the various positions in k-space is given in Figure 3.
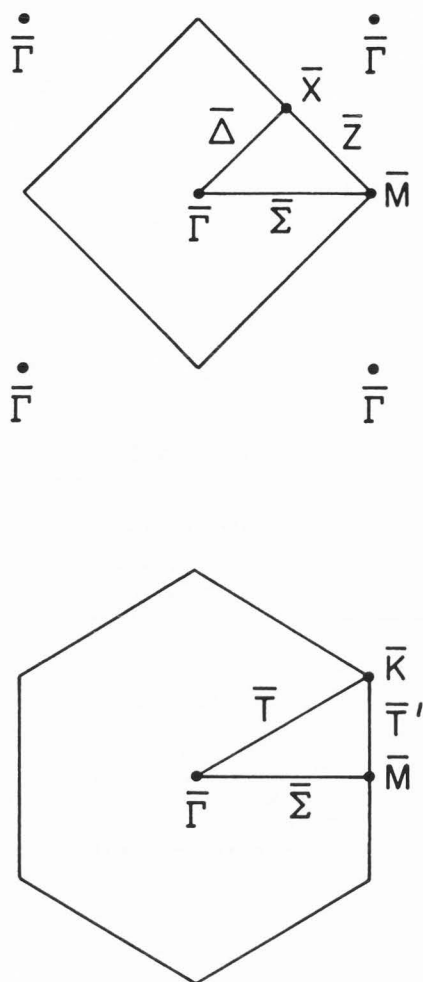
Figure 3. The high symmetry points and lines of the surface Brillouin zones of a C_{4v} or four fold symmetric surface (top) and a C_{6v} or six fold symmetric surface (bottom).

represent the initial state.

In order to extract the greatest possible amount of information using angle-resolved photoemission and to most directly test model systems and theoretical predictions, it is crucial to grow well-ordered single crystal overlayers. This means that layer by layer growth of the thin metal film overlayer on a crystalline substrate is essential. Other spectroscopies, such as angle integrated photoemission, or characteristic energy loss, while not as sensitive to the micro-structure of the lattice, also provide far less information about the electronic structure.

While photoemission tends to be regarded as a single electron excitation process, it may often be a many body process. Screening of the hole state by other electrons and scattering processes can affect the wave function of the outgoing electron. If the photon energy is sufficient to excite shallow core levels, this can result in strong resonances and satellite photoemission features that also are not indica-

tive of an "initial state" density of states [173-182]. Such satellite photoemission features can be quite intense and are quite abundant in metals like nickel [175].

It is difficult to obtain definitive information regarding the magnetism from photo-emission studies of the valence bands due to many body effects and other possible causes for splittings of valence bands. Though splittings of the d-band may be a result of the magnetic exchange splitting (for example the splitting of the d-band of iron), [183-190] the situation with regard to magnetism is much more unambiguous when the electron spin polarization is measured. Nonetheless, such experiments must be carefully done as the spin polarized electron final state may be the result of a many electron excitation that includes spin exchange or spin flip, [191] though some experimental studies may be used as an argument against "magnetic depolarization" effects [192-194]. Currently, the best experi-ments combine a magnetization measurement such as magneto-optic Kerr effect or surface magneto-optic Kerr effect (MOKE or SMOKE) [195-199] with angle resolved photoemission. Spin polarized angle resolved photoemission can also be used as a probe of the surface magnetic properties [40,46,112,176,196,200-202]. This technique combines angle resolved photoemission with a Mott detector [203] or some other electron spin detector [204].

Angle-resolved photoemission is, nonetheless, a powerful tool, particularly when combined with other surface science tools. The difficulties in making unambiguous assignments of photoemission features and uncertainties as to the degree of order and structure of the metal-metal heterostructures have often resulted in confusion and disarray within the discipline of electronic structure determinations of metal on metal overlayers. This field has nonetheless attracted a great deal of interest and consid-erable effort has been expended in this area as indicated in Table 1.

The Influence of Crystal Structure Upon the Overlayer Metal Electronic Structure

As indicated in the previous section, the band structure must be consistent with the crystal lattice. If a thin metal film overlayer grows pseudomorphically, then the band structure of the overlayer alters to be consistent with the new lattice. For example, Hg adsorbs on Ag(100) at 87 K epitaxially and adopts the f.c.c. lattice of the substrate [48,49]. Furthermore, with the deposition of Hg on Ag(100) at 89 K and ambient pressure of Hg less than 10^{-8} torr, the Hg over-layer does not amalgamate or interdiffuse with the substrate. For one and two monolayers of Hg adsorbed on the Ag(100) surface, a two dimen-sional band structure develops in odd geometry from the Hg 5d-like states. This experimentally determined band structure is shown in Figure 4.

The 1x1 Hg lattice (indicated by the LEED patterns in Figure 1) for one and two monolayers of Hg on Ag(100) is an artificial and metastable structure. The square lattice is not the natural

One Monolayer Hg on Ag (100)

Two Monolayers Hg on Ag (100)
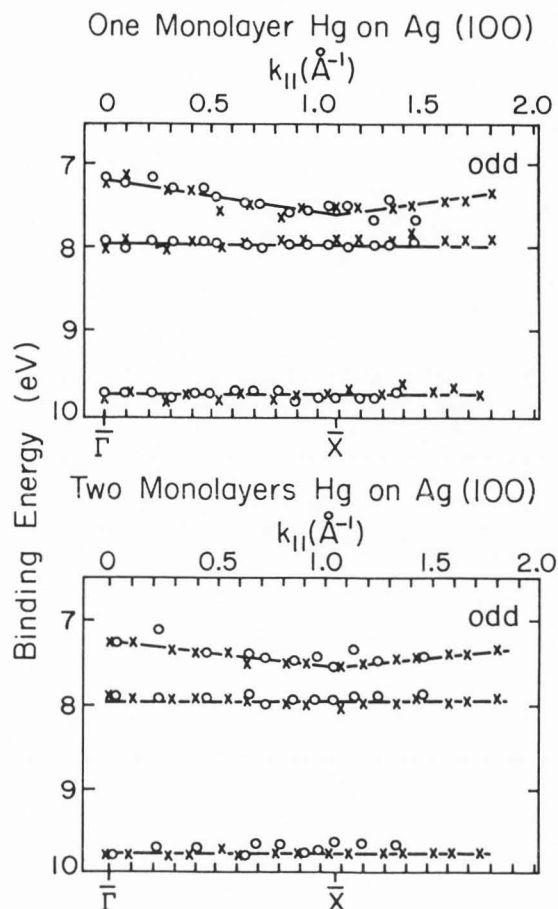
Figure 4. The experimental band structure of the Hg induced bands in odd geometry (odd symmetry with respect to the mirror plane) for one and two monolayers of Hg on Ag(100) at 87 K. Both thin film overlayers adopt the p(1x1) structure of the substrate. (o) indicates data for hν=36 eV and (x) indicates data for hν=50 eV.

(rhombohedral) crystal lattice of bulk mercury for which the nearest neighbor lattice constant is 3.004 A [205,206]. This is 3.8% greater than the 2.889 A lattice constant of the Ag(100) substrate. Weaire [207,208] and Heine and Weaire [209] point out that the Hg crystal structures exhibit an instability of the f.c.c. structure with respect to rhombohedral distortion and metastability with respect to tetragonal distortion. The energy of the f.c.c. Hg lattice is only slighly higher (0.01 eV/atom) than that of the rhombohedral lattice of bulk Hg, as shown by Worster and March [210]. Thus it is not surprising that Hg grows epitaxially on Ag(100) for one and two monolayers. Mercury adlayers also adopt the 1x1 crystal lattice on W(100) [52] and Fe(100) [51].

One of the unusual aspects of this band structure is the band that disperses from 7.2 eV binding energy at Γ̄ (normal emission) to 7.6 eV

at X̄ (the surface Brillouin zone edge). This new feature (as shown in Figure 5) is not observed with photoemission from solid Hg [211,212] or the gaseous vapor [212,213]. The results from investigations of the Hg adsorption on Ni(100) [214] and an Au polycrystalline surface [215] as well as solid Hg indicates that a thin Hg overlayer should induce two features due to the shallow $5d_{5/2}$ and $5d_{3/2}$ core levels. As shallow core levels these features should exhibit little or no dispersion. For one and two monolayers of Hg on Ag(100) at 89, the bands at 8.0±0.2 eV and 9.8±0.1 eV may be ascribed to states of character largely originating from the $5d_{5/2}$ and $5d_{3/2}$ spin orbit split doublet, respectively.

Adsorbed Monolayer of Hg
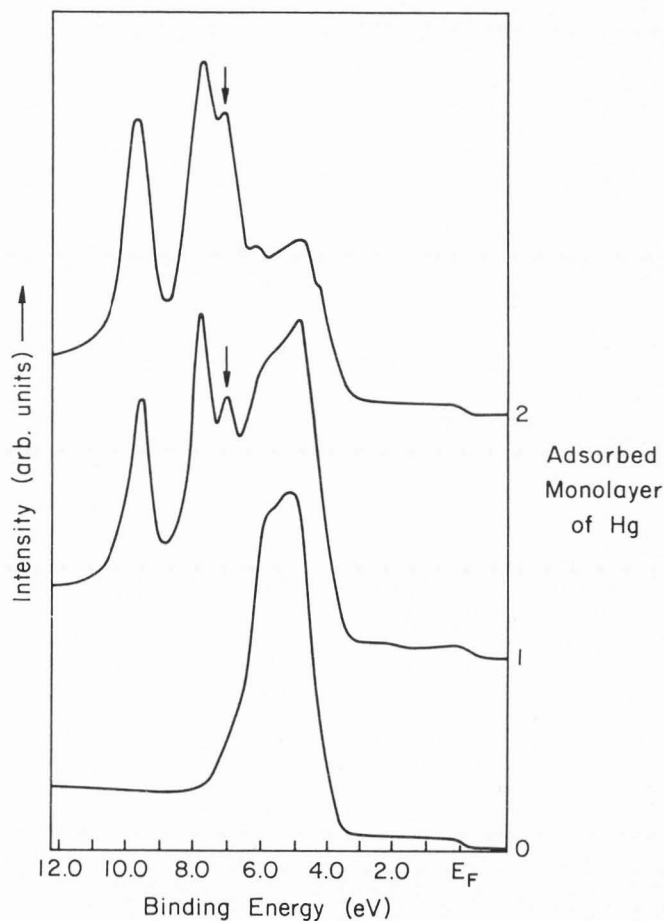
Figure 5. EDC's of the clean Ag(100) surface and following the deposition of one and two monolayers of Hg on Ag(100) at 87 K. For all spectra the photoelectrons are collected normal to the surface and the vector potential of the incident light is parallel to the surface and along Γ̄-X̄. The photon energy is 50 eV. The "split off" Hg $5d_{5/2}$ like orbital is indicated by an arrow.

The further splitting of the $5d_{5/2}$-like bands has also been observed with Hg adsorption on W(100) [216] and has been attributed to crystal field splitting [217] using arguments similar to those proposed by Herbst [218]. It has been shown, however, that this new feature for Hg on Ag(100) at 7.2±0.1 eV binding energy is not due to crystal field splitting but rather is a consequence of the band structure formed by the Hg overlayer [48,49]. The new feature appears only with coverages approaching one monolayer, and is consistent with a band structure formed from the hybridization of adjacent Hg atomic orbitals. The new feature is fully consistent with a two dimensional band structure in odd geometry, conserving $\underline{k}_{par}$ and remaining invariant to changes in $\underline{k}_{perp}$.

The square lattice alone cannot be responsible for the formation of the new Hg induced band at 7.2 to 7.6 eV binding energy. One and two monolayers adsorb on W(100), [51] Ni(100), [50], Cu(100) and Ag(100) also form a square lattice. Yet the new feature appears only with adsorption on W(100) [216] and Ag(100), although in the case of W(100) nothing is known about the dispersion of this feature. For the mercury overlayer on W(100) [51] and Ag(100), the nearest neighbor Hg-Hg atomic spacing is a 5.2% expansion and a 3.8% compression of the bulk Hg lattice spacing respectively. For Hg overlayers on Ni(100) [50] and Cu(100) the Hg-Hg atomic spacing is a 17.1% and 20.2% expansion of the bulk nearest neighbor spacing. Thus we can conclude that if the overlayer atoms are too far apart, hybridization between adjacent adatoms becomes very weak and the new band does not appear.

The hybridization of adjacent Hg atomic orbitals to form bands is not surprising in view of the close proximity of the Hg atoms in the overlayer lattice. A split off d-band has been observed with crystalline Zn, [219] a similar metal.

Another indication that long range crystallographic order is essential for forming the new Hg band comes from investigation of disordered Hg overlayers. By adsorbing Hg on Ag(100) at 30 K, an adlayer of mercury is deposited with considerable disorder. This overlayer fails to exhibit the new band at 7.2 eV binding energy (for normal emission) as shown in Figure 6. Melting of the two dimensional adlayer produces a similar effect (also shown in Figure 6), as well as changing the density of states between the Hg 5d bands and the Ag 5d bands. The loss of long range order does not result merely in an averaging of the density of states throughout k-space as one would expect, but changes the total density of states. A simple broadening of the band structure of the two dimensional Hg p(1x1) lattice with long range order will not reproduce the result of Figure 6.

In summarizing this section we can clearly see that metal on metal overlayers provide opportunities to explore not only the influence of crystal structure and reduced dimensionality upon band structure, but the consequences of altering lattice constants upon band structure.
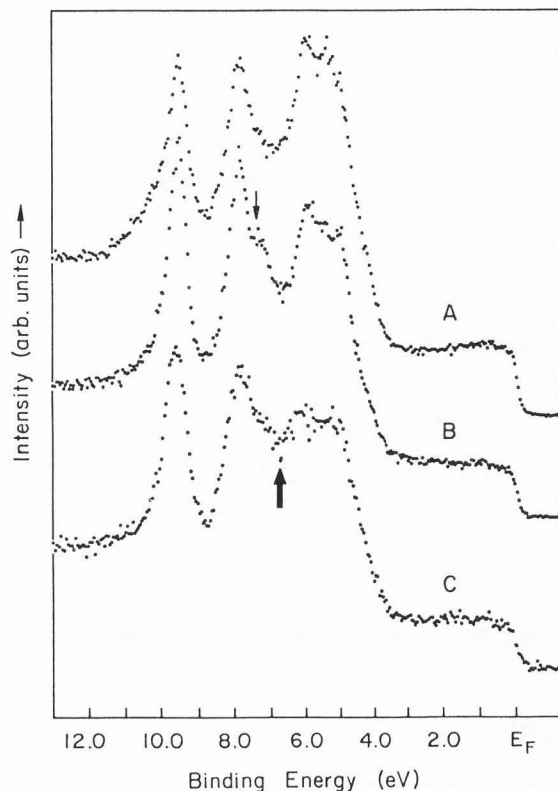
Figure 6. The EDC's of one monolayer of Hg on Ag(100) following adsorption at 30 K (A), after annealing the surface to above the Hg overlayer melting transition (B) and requenching the surface, and above the Hg overlayer melting transition (C). Note the appearance of a new feature after annealing (little arrow) and the change in the density of states between the Hg 5d bands and Ag 5d bands. (M. Onellion, J. L. Erskine, and P. A. Dowben).

Interface States

While silver is quite an inert metal, the close proximity of the even symmetry d-band states of silver with the Hg shallow core levels suggests that some mixing of the 5d states for the two metals will occur at the interface. Consequently, unusual electronic states are expected to form at the interface of Hg thin film deposited on Ag(100).

The emission angle dependence of the Hg-induced features for one and two monolayers of Hg, in even geometry, is quite different from that observed for odd geometry (described in the previous section). This has substantial implications, including that the band structure in even geometry is quite different from the band structure in odd geometry.

As indicated in Figure 7, in even geometry, the third Hg 5d feature present at 7.2±0.1 eV binding energy at $\overline{\Gamma}$ (normal emission) is not observed away from $\overline{\Gamma}$ (for emission angles away from the normal) for one ordered f.c.c. monolayer of Hg on Ag(100) at 89 K. For two monolayers of Hg this third 5d feature is observed at $\overline{\Gamma}$ and away from $\overline{\Gamma}$ but in contrast to odd geometry where this feature disperses symmetrically about $\overline{X}$, the feature in even geometry does disperse but not symmetrically about $\overline{X}$. Furthermore, in even geometry, the binding energy of this band changes with photon energy in the vicinity of $\overline{X}$.

There are further differences between even and odd geometry for two monolayers of f.c.c. Hg on Ag(100) at 89 K. Clean Ag(100) has a Δ_1
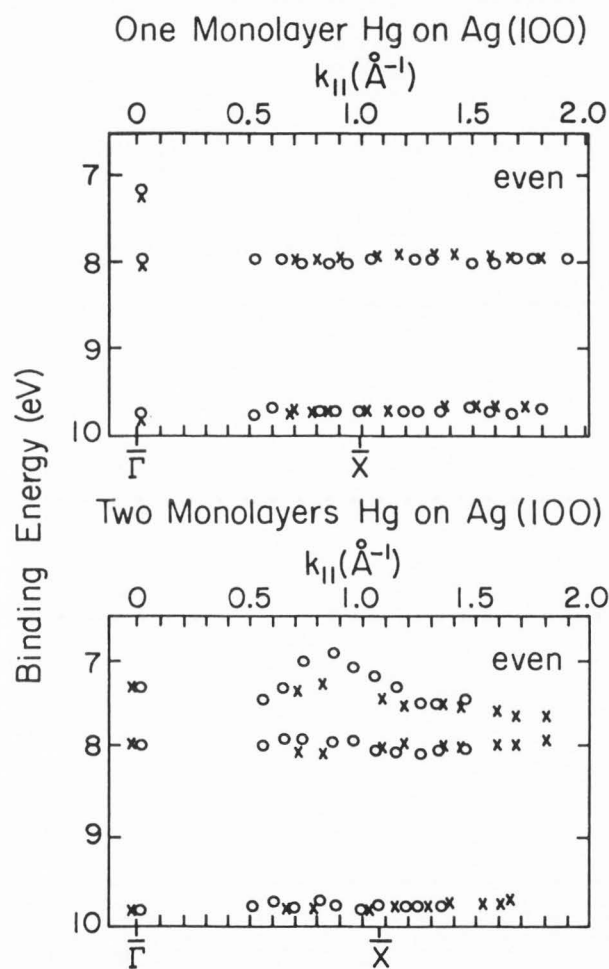
symmetry band near $\overline{X}$ that disperses above the Fermi energy along the $\overline{\Gamma}$-$\overline{X}$ line in even geometry. For two monolayers of Hg, this feature remains; in addition there is a satellite feature with 1.2 eV greater binding energy which disperses in a similar fashion to the Ag(100) band. As indicated in Figure 8, as with the Ag(100) band, this Hg induced band does not disperse symmetrically about $\overline{X}$ nor does this band remain independent of photon energy.

The Hg induced band structure in even geometry for two monolayers of Hg on Ag(100) is unusual and inconsistent with a two dimensional band structure. Two bands induced by Hg (as indicated above) do not disperse symmetrically about $\overline{X}$ and undergo dispersion that is strongly influenced by changes in photon energy. This demonstrates that these bands are not conserving the 2-dimensionality of state and appear to have the characteristics associated with bulk band structure. Two monolayers of Hg remain, nonetheless, of a thickness that is best described as a two dimensional overlayer. Thus the bulk-like band structure characteristics of the two monolayer Hg film on Ag(100) are suggestive of hybridization and the influence of the Ag(100) electronic states upon the Hg overlayer band structure.

We obtained photoemission spectra for clean Ag(100) and following the deposition of one and two monolayers of Hg. The majority of Ag derived photoemission features disperse in a similar fashion for clean Ag(100) and following the sub-

Figure 7. The experimental band structure for the Hg induced features in even geometry (even symmetry with respect to the mirror plane) for one and two monolayers of Hg on Ag(100) at 87 K. (o) indicates data taken with hν=36 eV and (x) indicates data taken with hν=50 eV. Note that there is a photon energy dependence of the bands.

Two Monolayers, Even Geometry
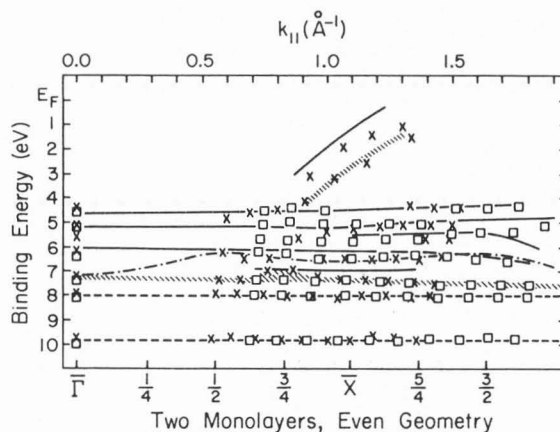
Figure 8. The experimental band structure for two monolayers of Hg in the p(1x1) structure on Ag(100) at 87 K. (x) indicates data points taken at hν=36 eV while (□) indicates data taken at hν=50 eV. The solid (——) lines indicate the clean Ag(100) bands derived experimentally while the dot-dashed lines indicate a theoretical Δ_1 from Reference [48, 256, 257]. The (/////) lines indicate Hg bands with some bulk like characteristics while the dashed lines (----) indicate Hg induced bands that preserve two dimensionality of state.

sequent deposition of one and two monolayers of Hg. Nonetheless, the Ag(100) bands are perturbed slightly, particularly in the vicinity of $\bar{X}$. These results also indicate that the Ag(100) electronic states are mixing with or are perturbed by the Hg electronic states.

The bulk-like band structure behavior of the Hg bands reflects the bulk band structure of the relevant Ag(100) bands. As discussed elsewhere, [48] the 5d Hg bands of Δ_5 symmetry are hybridizing with Ag(100) bands of Δ_1 symmetry [256,257] creating this interfacial electronic structure away from $\bar{\Gamma}$ in even geometry. Since Δ_1 symmetry states cannot be observed in odd geometry (Table 1) this mixing of Ag and Hg states does not occur in odd geometry. Thus despite the very weak chemical interactions between the Hg overlayer and the Ag(100) surface, the overlayer and the substrated electronic states do mix to form a distinct interfacial band structure away from $\bar{\Gamma}$ in even geometry.

The Influence of Structure on Thin Film Magnetism

Thin film ferromagnetism has begun to attract considerable interest, both theoretical and experimental. [9]. There are several fundamental questions that motivate the study of magnetism. The classic problems that pertain to the influence of the number of nearest neighbors, nearest neighbor spacings, and the density of states at the Fermi energy upon magnetism can be investigated anew for thin films because of the reduced dimensionality and potentially unusual crystal structures. In addition, the presence of a surface/interface permits the experimentalist to explore the effect of surface/interface states upon magnetism. With thin film metal overlayers, many examples of different classes of magnetic materials can be systematically investigated. Finally the effect of temperature upon thin film magnetism has only just begun to be studied.

A number of studies have been conducted to investigate thin (less than three monolayers) films of ferromagnetic materials [23,40,41,46,89,112,199,220-230]. It is known that impurity incorporation, compound formation, and interdiffusion can influence the magnetism of a thin film, in addition to the effects of the film thickness, nearest neighbor spacings, coordination of the overlayer atoms and the influence of the substrate. Unfortunately some investigations of thin film magnetism were not able to obtain structural information hampering efforts to interpret their results. For all thin films, magnetic and non-magnetic alike, as the thin film thickness increases, the film develops the magnetic properties of the bulk.

As the film thickness increases, not only does the elemental magnetic thin film begin to develop the ferromagnetic properties of the bulk material, but the orientation easy magnetization vector has been observed to change. This change in the orientation of the magnetization vector has been observed with Fe films deposited on W(100) [46] and on GaAs(100) [112]. Indeed, the surface crystal structure and anisotropy of the magnetism may result in unusual orientations of the magnetization vector though little work has been done in this area.

Theoretical predictions [231] indicate that the ferromagnetic properites of the principal ferromagnets, iron, cobalt and nickel, depend strongly upon crystal structure and lattice spacing. There is a pronounced difference between the ferromagnetism of f.c.c. and b.c.c. iron and nickel and between b.c.c. or f.c.c. cobalt and its natural h.c.p. lattice. There is, therefore, considerable appeal in investigating f.c.c. iron (or b.c.c. nickel) with a wide variety of lattice constants. Single crystal substrates provide ideal templates for growing iron, nickel or cobalt in unusual crystal structures. Iron has recently been shown to adopt the f.c.c. structure of a Cu(100) substrate when deposited as a thin film overlayer [42]. As yet there is no conclusive evidence as to whether the iron overlayer on Cu(100) is ferromagnetic. The situation is complicated by the Fe-Fe nearest neighbor spacing. Iron on Cu(100) has a nearest neighbor spacing close to the boundary between ferromagnetic and paramagnetic order [231]. Studies are in progress in several laboratories to investigate this system.

The magnetization of a thin film overlayer can also influence the structure of the thin film. Thin Co films deposition on Cu(100) adopt the f.c.c. lattice of the substrate but because this is not the natural h.c.p. lattice of bulk ferromagnetic cobalt, the thin film reconstructs into a c(2x2) superlattice [23]. This reconstruction is believed to be driven by a ferromagnetic induced charge density wave [23]. Similar reconstructions have been commonly observed for Mo(100) [232] and W(100) [233-234]. For Cr(100), [235-239] Mo(100), [232] and W(100) [233-234] there is a high density of surface states near the Fermi energy that dominates the surface properties of these metals. As with the cobalt thin film on Cu(100), a charge density wave induces a periodic reconstruction of the surface into a c(2x2) superlattice as a result of nesting of the Fermi surface of Mo(100) [232] and W(100) [233-234]. It is the result, such as the one observed for cobalt thin films, that points to the strong interrelationship between magnetism and electronic structure.

The photoemission derived density of states alone can provide some indication of the thin film magnetism (though not unequivocally). The exchange splitting of the majority and minority spin states appears in the EDC, typically as a "split" d-band; that is, the d-band can often be resolved into two distinct features in a magnetic thin film [227]. Such a "split" d-band does not, however, conclusively establish magnetic order.

The substrate can have a profound influence on the magnetic properties of a thin film overlayer not only by forcing the thin film overlayer into new structures, but also by inducing a magnetic moment. Materials not commonly thought of as magnetic can become magnetic when deposited on an appropriate substrate. Several systems are currently candidates for such behavior, including vanadium on Ag(100) [240] and palladium deposited on Ni(111) [230].

THE INFLUENCE OF METAL SUBSTRATES ON THE ELECTRONIC STATES OF METAL OVERLAYERS

Conclusion

Hg overlayers on Ag(100) adopts the f.c.c lattice of the substrate, with the Hg adatom orbitals hybridizing to form a two dimensional band structure for very thin (less than three monolayers) films. The hybridization of Hg bands with the Ag(100) bulk states creates states that are an admixture of Hg and Ag states. The resulting interfacial states may extend several atomic diameters (in the direction normal to the interface) in each direction away from the interface. The two dimensional electronic structure of the Hg overlayer and the interface states include electronic structure that is not part of the electronic structure of either bulk Hg or Ag. Similar developments in the electronic structure are expected for many other metal thin film overlayers.

The pioneering work in this area has, unfortunately, not included all the structural studies that appear necessary for a good understanding of thin film overlayer magnetism and electronic structure. To obtain reliable information about magnetism and electronic structure requires a number of spectroscopies and characterization probes not commonly available together on a single experimental system. Nonetheless, the investigation of metallic thin film overlayers, now increasingly includes the characterization of the thin film electronic and magnetic properties. Electronic structure has been implicated in a number of fundamental properties of bimetallic systems, and future work is in progress to correlate electronic structure with catalytic reactivity, as well as magnetism.

The electronic structure of thin film overlayers also appears to have a profound influence on properties normally thought to be atomic in nature such as the photoemission cross-section of the core levels. Recently, sharp increases in the relative photoemission cross-section of the $5d_{5/2}$ Hg orbital have been observed [182,241] that have no counterpart in the relative photoemission cross-section of gaseous mercury [213,242-250]. The distinctive features of the relative photoemission cross-section of thin films of Hg have recently been shown to be dependent upon the structure of the thin film. New effects of structure and possibly electronic structure such as this will be increasingly explored in future investigations.

Acknowledgments

References

[1] Bauer E (1982) The structure of clean surfaces. In: Interfacial Aspects of Phase Transformations, B. Mutaftschiev, Ed., D. Reidel Publishing Co., Boston.

[2] Falco CM, Schuller IK (1985) Electronic and magnetic properties of metallic superlattices. In: Synthetic Modulated Structures, L. L. Chang and B. C. Giessen eds., Academic Press, London, 339-364.

[3] Ruggiero ST, Beasley MR (1985) Synthetically layered superconductors In: Synthetic Modulated Structures, L. L. Chang and B. C. Giessen eds., Academic Press, London, 365-417.

[4] Dash JG, Rubalds J, eds. (1979) Phase Transitions in Surface Films, Plenum Press, New York.

[5] Bauer E (1982) Epitaxy of metals on metals., Appl. Surf. Sci. 11-12, 479-494.

[6] Bauer E (1975) Metals on metals. In: The Chemical Physics of Solid Surfaces and Heterogeneous Catalysis, Vol. 3, D. A. King and D. P. Woodruff eds., Elsevier Press, 1-51.

[7] Vook RW (1982) The structure and growth of thin film., Internat. Metals Rev. 27, 209-245.

[8] Matthews JW, ed., (1975) Epitaxial Growth, A,B; Academic Press.

[9] Erskine JL, Onellion MF, Thompson MA (1987) Exploring magnetic properties of epitaxial films and superlattices. Materials Research Symposium, in press.

[10] Dowben PA, Miller A, Vook RW (1987) Surface segregation from gold alloys. Gold Bulletin, in press.

[11] Vahalia U, Dowben P, Miller A (1986) Surface segregation in binary alloys. J. Vac. Sci. & Technol. A4, 1675-1679.

[12] Vahalia U, Dowben PA, Miller A (1986) Surface segregation in binary alloys: a semi-empirical approach. J. Electron Spectrosc. & Relat. Phenom. 37, 303-318.

[13] Tobin JG, Robey SW, Shirley DA (1986) Two-dimensional valence-electronic structure of a monolayer of Ag on Cu(001). Phys. Rev. B33, 2270-2280.

[14] Tobin JG, Robey SW, Klebanhoff LE, Shirley DA (1983) Ag/Cu(001): Observations of the development of the electronic structure in metal overlayers from two to three dimensionality. Phys. Rev. B28, 6169-6171.

[15] Kolaczkiewicz J, Bauer E (1984) The adsorption of Ag and Au on W(211) surfaces. Surf. Sci. 144, 477-494.

[16] Culbertson RJ, Feldman LC, Silverman, PJ (1981) of Au on Ag(111) studied by high-energy ion scattering. Phys. Rev. Lett. 47, 657-660.

[17] Salmeron M, Ferrer S, Jazzar M, Somorjai, G.A. (1983) Photoelectron- spectroscopy study of the electronic structure of Au and Ag overlayers on Pt(100), Pt(111), and Pt(997) surfaces. Phys. Rev. B28, 6758-6765.

[18] Harendt C, Cristmann K, Hirschwald W, Vickerman JC (1986) Model bimetallic catalyst : the preparation and characterization of Au/Ru(0001) surfaces and the adsorption of carbonmonoxide. Surf. Sci. 165, 413-433.

[19] Graham GW (1985) Quenching of a surface state of W(100) by adsorption of Au. Phys. Rev. B32, 2640-2642.

[20] Bauer E, Poppa H, Todd G, Davis PR (1977) The adsorption and early stages of condensation of Ag and Au on W single-crystal surfaces. J. Appl. Phys. 48, 3773-3787.

[21] Mroz S, Bauer E (1986) The interaction of gold with the surface of a cylindrical tungsten single crystal. Surf. Sci. 169, 394-404.

[22] Richter L, Gomer R (1976) Effect of Au adsorption on the tungsten (100) surface state. Phys. Rev. Lett. 37, 763-765.

[23] Gonzalez L, Miranda R, Salmeron M. Vergas JA and Yndurain F (1981) Experimental and theoretical study of Co adsorbed at the surface of Cu: reconstructions, charge-density waves, surface magnetism, and oxygen adsorption. Phys. Rev. B24, 3245-3254.

[24] Chandesris D, Roubin R, Rossi G, Lecante J, (1986) Crystallographic properties and adsorbate geometries by surface EXAFS. Surf. Sci. 169, 57-70.

[25] Argile C, Rhead GE (1978) Preparation and properties of binary metal monolayers. I. Pb and Bi on Cu(100). Surf. Sci. 78, 115-124.

[26] Zajac G, Bader SD, Friddle RJ (1985) Epitaxy and electronic structure of p(1X1) Cr/Ar(100). Phys. Rev. B31, 4947-4953.

[27] Stoffel NG, Kevan SD, Smith NV (1985) Experimental band structure of ordered Cu overlayers on Ag(001). Phys. Rev. B32, 5038-5043.

[28] Smith GC, Norris C, Binns C (1984) Angle-resolved photoemission from a copper monolayer on silver (100). J. Phys. C17, 4389-4397.

[29] Asonen H, Barnes CJ, Salokatve A, Pessa M (1985) The effect of interdiffusion on the growth mode of copper on Al(111). Surf. Sci. 152/153, pt. 1, 262-269.

[30] El-Batonouny M (1985) Structural and electronic trends in the growth of Cu overlayers on the Nb(110) surface. Phys. Rev. B31, 4798-4801.

[31] Chambers A, Jackson DC (1975) The growth and structure of thin copper films on (001) surfaces and nickel. Philos. Mag. 31, 1357-1371.

[32] Nilsson A, Morris MA, Chadwick D (1985) Growth and properties of Cu on Ni(100). Surf. Sci. 152/153, pt. 1, 247-253.

[33] Chambers SA, Chen HW, Vitomirov IM, Anderson SB, Weaver JH (1986) Direct observation of elastic strain andd relaxation at a metal-metal interface by Auger electron diffraction: Cu/Ni(001). Phys. Rev. B33, 8810-8813.

[34] Asonen H, Barnes C, Salokatve A, Vuoristo A (1985) The growth mode of Cu overlayers on Pd(100). Appl. Surf. Sci. Vol. 22-23, pt. 2, 556-564.

[35] Barnes CJ, Lindroos M, Pessa M (1985) The growth mode and electronic structure of copper overlayers on Pd(100) and Pt(100). Surf. Sci. 152/153, pt. 1, 260-261.

[36] Shek ML, Stefan PM, Lindau I, Spicer WE (1983) Photoemission study of the adsorption of Cu on Pt(111). Phys. Rev. B27, 7277-7287.

[37] Shek ML, Stefan PM, Lindau I, Spicer WE (1983) Electronic structure of different Pt -Cu surfaces. Phys. Rev. B27, 7288-7300.

[38] Houston JE, Peden CHF, Feibelman PJ, Hamann DR (1986) Observation of a true interface state in strained-layer Cu adsorption of Ru(0001). Phys. Rev. Lett. 56, 375-377.

[39] Smith GC, Padmore HA, Norris C (1982) The Growth of Fe overlayers on Ag(100). Surf. Sci. 119, 287-291.

[40] Jonker BT, Walker KH, Kisker E, Prinz GA, Carbone C (1986) Spin polarized photoemission study of epitaxial Fe(001) films on Ag(001). Phys. Rev. Lett. 57, 142-145.

[41] Onellion MF, Fu CL, Thompson MA, Erskine JL, Freeman AJ (1986) Electronic structure and properties of epitaxial Fe on Cu(100): theory and experiment. Phys. Rev. B33, 7322-7325.

[42] Onellion M, Thompson MA, Erskine JL, Duke CB, Paton A (1987) Epitaxial growth of fcc Fe on Cu(100). Surf. Sci. 79, 219-229.

[43] Gradmann U, Tillmanns P (1977) Supersaturation and mode of growth for Fe films on Cu(111). An experimental study using LEED and AES. Phys. Status Solidi A44, 539-547.

[44] Wiartalla W, Becker W, Keune W, Pfannes HD (1984) Structural and Mossbauer Investigation of Epitaxial Cu/gamma - Fe/Cu sandwich layers. J. Phys. Colloq. 45, 461-464.

[45] Lee YC, Min H, Montano PA (1986) An electron energy loss study of the epitaxial growth of iron and Cu(100). Surf. Sci. 166, 391-402.

[46] Kurzawa R, Kamper KP, Schmitt W, Guntherodt G (1986) Spin-resolved photoemission study of in situ grown epitaxial Fe layers on W(110). Solid State Commun. 60, 777-780.

[47] Gradmann U, Waller G (1982) Periodic lattice distortions in epitaxial films of Fe(110) on W(110). Surf. Sci. 116, 539-548.

[48] Dowben PA, Kime YJ, Varma S, Onellion M, Erskine JL (1987) Interaction of Hg overlayers with an Ag(100) surface. Phys. Rev. B36.

[49] Onellion M, Erskine JL, Kime YJ, Varma S, Dowben PA (1986) Structure- induced electronic states for Hg over-layer on Ag(100). Phys. Rev. B33, 8833-8836.

[50] Jones RG, Tong AWL (1987) Mercury adsorption on Ni(100). Surf. Sci. in press.

[51] Jones RG, Perry DL (1981) The chemisorption of mercury on Fe(100): adsorption and desorption kinetics, equilibrium properties and surface structure. Vacuum 31, 493-498.

[52] Jones RG, Perry DL (1978) The chemisorption of mercury on tungsten (100): Adsorption and desorption kinetics, equilibrium properties and surface structure. Surf. Sci. 71, 59-74.

[53] Jones RG, Perry DL (1979) Fractional and zero order desorption kinetics of adsorbed monolayers: the role of attractive lateral interactions in the Hg/W(100) system. Surf. Sci. 82, 540-548.

[54] Abu-Joudah MA, Davies BM, Montano PA (1986) LEED, Auger, and electron energy loss studies of Ni epitaxially grown on Cu(100). Surf. Sci. 171, 331-348.

[55] Gradmann U (1969) Pseudomorphic growth of Ni on Cu. Surf. Sci. 13, 498-501.

[56] Hague CA, Farnsworth HE (1966) LEED observations of calibrated epitaxial nickel films on (111) copper. Surf. Sci. 4, 195-200.

[57] Kolaczkiewicz J, Bauer E (1984) The adsorption of Ag and Au on W(211) surfaces. Surf. Sci. 144, 495-511.

[58] Rawlings KJ, Gibson MJ, Dobson PJ (1978) The epitaxial growth of lead and thallium on (111) silver and copper. J. Phys. D11, 2059-2070.

[59] Takayanagi K, Kolb DM, Kambe K, Lehmpfuhl G (1980) Deposition of monolayer and bulk lead on Ag(111) studied in vacuum and in an electrochemical cell. Surf. Sci. 100, 407-422.

[60] Argile C, Rhead GE (1978) Preparation and properties of binary metal monolayers. II. Pb and Sn on Al(100). Surf. Sci. 78, 125-140.

[61] Hosler W, Moritz W (1986) LEED analysis of a dense lead monolayer on copper (100). Surf. Sci. 175, 63-77.

[62] Gurtler K, Jacobi K (1983) Coverage and adsorption-site dependence of core-level binding energies for tin and lead on Al(111) and Ni(111). Surf. Sci. 134, 309-328.

[63] Sepulveda A, Rhead GE (1977) Auger electron spectroscopy of adsorbed metal monolayers. Lead on low index and stepped copper surfaces. Surf. Sci. 66, 436-448.

[64] Henrion J, Rhead GE (1972) LEED studies on the first stages of deposition and melting of lead on low index faces of copper. Surf. Sci. 29, 20-36.

[65] Barthes MG, Rhead GE (1979) Adsorption and desorption of lead on low-index and stepped copper surfaces. Surf. Sci. 80, 421-429.

[66] Schardt BC, Stickney JL, Stern DA, Wieckowski A, Zapien DC, Hubbard AT (1986) Electrodeposition of Pb onto Pt(111) in aqueous chloride solutions: Studies by LEED and Auger spectroscopy. Surf. Sci. 175, 520-534.

[67] Bauer E, Poppa H, Todd G (1975) The early stages of condensation of lead on tungsten. Thin Solid Films 28, 19-36.

[68] Smith GC, Norris C, Binns C, Padmore HA (1982) A photoemission study of ultrathin palladium overlayers on low index faces of silver. J. Phys. C15, 6481-6496.

[69] Xinyin S, Frankel DJ, Hermanson JC, Lapeyre GJ, Smith RJ (1985) Photoemission studies of ordered Pd overlayers on Au(111); implications for CO chemisorption. Phys. Rev. B32, 2120-2125.

[70] Pessa M, Jylha O (1983) Electronic structure evolution of Pd overlayers on Cu. Solid State Commun. 46, 419-422.

[71] Sagurten M, Strongin M, Jona F, Colbert J (1983) Observation of a first order structural phase transition in a monolayer of Pd on Nb(110) and its relationship to electronic structure. Phys. Rev. B28, 4075-4079.

[72] Prigge S, Roux H, Bauer E (1981) Pd layers on a W(100) surface. Surf. Sci. 107, 101-112.

[73] Argile C, Rhead GE (1980) Growth and structure of monolayers and double layers of lead and tin on aluminum (111). Thin Solid Films 67, 299-308.

[74] Kawazu A, Akimoto K, Oyama T, Tominage G (1981) Adsorption of Ge atoms on Si(111) surfaces. Proceed. 4th International Conf. on Solid Surfaces (1980), Societe Francaise du Vide 2, 1015-1022.

[75] Takayanagi K (1981) Ultra-high vacuum transmission electron microscopy on the monolayer condensation process of lead on silver (111) surface. Surf. Sci. 104, 527-548.

[76] Biberian JP (1978) LEED and AES study of the Au/AuPb₂ interface. Surf. Sci. 74, 437-460.

[77] Perdereau J, Biberian JP, Rhead GE (1974) Adsorption and surface alloying of lead monolayers on (111) and (110) faces of gold. J. Phys. F4, 798-806.

[78] Snyman HC, Boswell FW (1974) Intermetallic compound formation at the interface in the lead-(111) gold system. Surf. Sci. 41, 21-44.

[79] Biberian JP, Rhead GE (1973) Spontaneous alloying of a gold substrate with lead monolayers. J. Phys. F3, 675-682.

[80] Green AK, Prigge S, Bauer E (1978) The condensation of lead on a gold surface. Thin Solid Films 52, 163-179.

[81] Bauer E (1967) Multiple scattering versus superstructures in low energy electron diffraction. Surf. Sci. 7, 351-364.

[82] Palmberg PW, Rhodin TN (1968) Atomic arrangement of Au(100) and related metal overlayer surface structures. J. Chem. Phys. 49, 134-146.

[83] Vook RW, Chao SS (1979) Misfit dislocations in (001)Cu/(111)Ag epitaxial bilayers. Thin Solid Films 58, 203-207.

[84] Vook RW (1979) Epitaxy and misfit dislocations in large misfit systems. Thin Solid Films 64, 91-102.

[85] Paffett MT, Campbell CT, Taylor TN, Srinivasan S (1985) Cu adsorption on Pt(111) and its effects on chemisorption: a comparison with electrochemistry. Surf. Sci. 154, 284-302.

[86] Zei MS, Nakai Y, Weick D, Lehmpfuhl G (1985) A LEED and RHEED investigation of a perfect and a distorted Cu adlayer on Au(111). Surf. Sci. 152/153, pt. 1, 254-259.

[87] Gradmann U (1964) Versetzungsstruktur und Gitteranggleichung in epitakischen Flachenschichten. Ann. Physik, 7 Folge, 13, 213-216.

[88] Gradmann U (1966) Struktur und Ferromagnetismus sehr dunner epitakischer Ni-Flachenschichten. Ann. Physik, 7 Folge 17, p91-106.

[89] Prinz GA (1985) Stabilization of BCC Co via epitaxial growth on GaAs. Phys. Rev. Lett. 54, 1051-1054.

[90] Sewell PB, Cohen M, Mitchell DF (1967) Electron optical characterization of metal surfaces in: Surfaces and Interfaces I: Chemical and Physical Characteristics, J. J. Burke et al. Eds, Syracuse University Press 53-76.

[91] Narusawa T, Shimizu S., Komiya S (1979) Simultaneous RHEED/AES study of Si film growth on Si(111) and sapphire (1102) surfaces. Surf. Sci. 86, 572-580.

[92] Menadue JF (1972) Si(111) surface structures by glancing incidence high-energy electron diffraction. Acta. Crystal. A28, 1-11.

[93] LeLay G, Quentel G, Faurie JP, Masson A (1976) Epitaxy of noble metals and (111) surface superstructures of silicon and germanium. I. Study at room temperature. Thin Solid Films 35, 273-287.

[94] LeLay G, Quentel G, Faurie JP, Masson A (1976) Epitaxy of noble metals and (111) surface superstructures of silicon and germanium. II. Study after annealing. Thin Solid Films 35, 289-303.

[95] Ino S (1977) Some new techniques in reflection high energy electron diffraction (RHEED): Application to surface structure studies. Jpn. J. Appl. Phys. 16, 891-908.

[96] Ichikawa T, Ino S (1978) Ge(111) 7x7 surface structure induced by Sn. Solid State Commun. 27, 483-486.

[97] Ino S (1978) Some new diffraction phenomena in reflection high energy electron diffraction of clean silicon (111) surfaces. Jpn. J. Appl. Phys. 17, 1121-1122.

[98] Ichikawa T, Ino S (1980) Missing spots in RHEED patterns from the Si(111) 6x1-Ag surface structure. Surf. Sci. 97, 489-502.

[99] Ichikawa T, Ino S (1980) Diffuse scattering from Ge(111) surface at high temperature. Solid State Commun. 34, 349-353.

[100] Ino S (1980) A new structure model for the Si(111) 7x7 surface structure. Jpn. J. Appl. Phys. 19, L61-64.

[101] Ino S (1980) An investigation of the Si(111) 7x7 surface structure by RHEED. Jpn. J. Appl. Phys. 19, 1277-1290.

[102] Ino S, Ichikawa T, Okada S (1980) Chemical analysis of surface by fluorescent x-ray spectroscopy using RHEED-SSD method. Jpn. J. Appl. Phys. 19, 1451-1457.

[103] Gotoh Y, Ino S (1978) Surface structures of Ag on Si(111) surface investigated by RHEED. Jpn. J. Appl. Phys. 17, 2097-2109.

[104] Aiyama T, Ino S (1979) RHEED observation of the Si(111) (3x3) R + 9° - In structure. Surf. Sci. 82, L585-588.

[105] Marra WC, Fouss PH, Eisenberger PE (1982) X-ray diffraction studies: melting of Pb monolayers on Cu(110). Phys. Rev. Lett. 49, 1169-1172.

[106] Namba Y, Vook RW (1981) Auger analysis of thick silver films and of silver layers grown on copper. Thin Solid Films 82, 165-177.

[107] Kuntze R, Chambers A, Prutton M (1969) Pseudomorphism in the (100) Ni-Cu system. Thin Solid Films 4, 47-60.

[108] Lassen H (1934) Flachengitterinterferenzen mit Elektronen-strahlen an dunnen Silberschichten. Physik. Zeit. 35, 172-175.

[109] Lassen H, Bruck L (1935) Herstellung von dunnen Silberein-kristallen und ihre Untersuchen mit Elektronenstrahlen. Ann. Physik, 5 Folge, 22, 65-72.

[110] Lassen H, Bruck L (1935) Erwirderung zu der vorstehenden Bemerkung von Herrn L. Royer zu unserrer arbeit Herrstellung von dunnen Silbereinkristallen und ihre Untersuchen mit Elektronenstrahlen. Ann. Physik, 5 Folge, 23, 18-20.

[111] Bruch L (1936) Die Struktur dunner auf Steinsalz aufgedampfter Metallschichten. Ann. Physik, 5 Folge, 26, 233-257.

[112] Schroder K, Prinz GA, Walker KH, Kisker E (1985) Spin and angle-resolved photoemission study of (110) Fe films grown on GaAs by molecular beam epitaxy. J. Appl. Phys. 57, 3669-3671.

[113] Brennan S, Fuoss PH, Eisenberger P (1986) X-ray crystallographic studies of Pb monolayers on Cu(110) surfaces. Phys. Rev. B33, 3678-3683.

[114] Hosoito N, Kawaguchi K, Shinjo T, Takada T, Endoh Y (1984) Magnetic properties of Fe-V multilayered films with artificial superstructures. J. Phys. Soc. Jpn. 53, 2659-2667.

[115] Osakabe N, Tanishiro Y, Yagi K, Honjo G (1980) Reflection electron microscopy of clean and gold deposited (111) silicon surfaces. Surf. Sci. 97, 393-408.

[116] Yagi K, Takayanagi K, Kobayashi K, Osakabe N, Tanishiro Y, Honjo G (1978) Surface study by an UHV electron microscope. Proc. 9th Int. Cong. for Electron Microscopy, 1, Microscopical Society of Canada, Toronto, 458-459.

[117] Yagi K, Takayanagi K, Kobayashi K, Osakabe N, Tanishiro Y, Honjo G (1979) Surface study by an UHV electron microscope. Surf. Sci. 86, 174-181.

[118] Takayanagi K, Honjo G (1981) UHV-TEM investigation of monolayer adsorbate of lead on silver (111) surface. Proc. 4th Int. Conf. on Solid Surfaces. (1980) Societe Francais du Vide 1, 267-270.

[119] Tanishiro Y, Kanamori H, Takayanagi K, Kobayashi K, Yagi K, Honjo G (1981) Electron microscope study of reconstructed (111) gold surface. Proc. 4th Int. Conf. on Solid Surfaces (1980) Societe Francais du Vide 1, 683-686.

[120] Yagi K, Osakabe N, Tanishiro Y, Hongo G (1981) Reflection electron microscope study of Au and Ag deposited (111) and (001) Si surfaces. Proc. 4th Int. Conf. on Solid Surfaces (1980) Societe Francais du Vide 2, 1007-1010.

[121] Osakabe N, Yagi K, Honjo G (1980) Reflection electron microscope observations of dislocations and surface structure phase transition on clean (111) silicon surfaces. Jpn. J. Appl. Phys. 19, L309-312.

[122] Roubin P, Chandesris D, Rossi G, Lecante J, Desjonqueres MC, Treglia G (1986) Experimental and theoretical evidence for a strong anisotropy of the surface Debye-Waller factor as determined for a monolayer of cobalt on copper (111) by surface extended x-ray adsorption fine structure. Phys. Rev. Lett. 56, 1272-1275.

[123] Chambers SA, Anderson SB, Weaver JH (1985) Atomic structure of the Cu/Si(111) interface by high-energy core-level Auger electron diffraction. Phys. Rev. B32, 581-587.

[124] Egelhoff Jr WF (1984) Growth morphology determination in the initial stages of epitaxy by XPS. J. Vac. Sci. & Technol. A2, 350-352.

[125] Egelhoff Jr WF (1984) X-ray photoelectron and Auger-electron forward scattering: a new tool for studying epitaxial growth and core-level

binding-energy shifts. Phys. Rev. B30, 1052-1055.

[126] Egelhoff Jr WF (1985) A new tool studying epitaxy and interfaces: the XPS searchlight effect. J. Vac. Sci. & Tech. 3, 1511-1513.

[127] Armstrong RA, Egelhoff Jr WF (1985) An analysis of angular dependent XPS peak intensities. Surf. Sci. 154, L225-232.

[128] Kono S, Fadley CS, Hall NTF, Hussain Z (1978) Azimuthal anisotropy in deep core level x-ray photo emission from an adsorbed atom: Oxygen on copper (001). Phys. Rev. Lett. 41, 117-120.

[129] Chambers SA, Swanson LW (1983) Angle-resolved Auger electron emission from LaB$_6$(001) with and without chemisorbed oxygen. Surf. Sci. 131, 385-402.

[130] Takahashi S, Kono S, Sakurai H, Sagawa T (1982) Kinematical interpretation of Auger electron and x-ray photoelectron diffraction from Ag(110) surface., J. Phys. Soc. Jpn. 51, 3296-3301.

[131] Poon HC, Tong SY (1984) Focusing and diffraction effects in angle-resolved x-ray photoelectron spectroscopy. Phys. Rev. B30, 6211-6213.

[132] Tong SY, Poon HC, Snider DR (1985) Importance of multiple forward scattering in medium- and high-energy electron emission and/or diffraction spectroscopies. Phys. Rev. B32, 2096-2100.

[133] Poon HC, Snider D, Tong SY (1986) Small-atom approximation in forward- and back-scattering photoelectron spectroscopies. Phys. Rev. B33, 2198-2206.

[134] Bullock EL, Fadley CS (1985) Determination of epitaxial overlayer structures from high-energy electron scattering and diffraction. Phys. Rev. B31, 1212-1215.

[135] Egelhoff Jr WF (1985) The XPS searchlight effect: a new analytical tool for layered structures, epitaxy, and interfaces. in: Layered Structures Epitaxy and Interfaces. J. M.Gibson and L. R. Dawson Eds., North Holland, Amsterdam, 443-447.

[136] Chambers SA, Greenlee TR, Smith CP, Weaver JH (1985) Quantitative characterization of abrupt interfaces by angle-resolved Auger electron emission. Phys. Rev. B32, 4245-4248.

[137] Barthes-Labrousse MG, Rhead GE (1982) A simple method for surface and ultrathin film characterization. Surf. Sci. 116, 217-224.

[138] Chao SS, Knabbe EA, Vook RW (1980) Auger line shape changes in epitaxial (111)Pd/(111)Cu films. Surf. Sci. 100, 581-589.

[139] Chao SS, Vook RW, Namba Y (1981) Thickness periodicity in the Auger line shapes from epitaxial (111)Pd/(111)Cu films. J. Vac.-Sci. & Technol. 18, 695-699.

[140] Namba Y, Vook RW, Chao SS (1981) Thickness periodicity in the Auger line shape from epitaxial (111)Cu films. Surf. Sci. 109, 320-330.

[141] Faldt A, Meyers HP (1984) Mixed valence in Sm overlayers on A1(100). Phys. Rev. B30, 5481-5486.

[142] Faldt A, Meyers HP (1984) Homogeneous intermediate valence of Sm on Cu(001). Phys. Rev. Lett. 52, 1315-1317.

[143] Ferrer S, Salmeron M, Ocal C, Roubin P, Lecante J (1985) Core level photoemission study of Au deposited on Pt(111) in the sub-monolayer range. Surf. Sci. 160, L488-492.

[144] Egelhoff Jr WF (1983) Thermochemical values for Cu-Ni surface and interface segregation deduced from core-level binding energy shifts. Phys. Rev. Lett. 50, 587-590.

[145] Gurtler K, Jacobi K (1985) Coverage-dependence of Pb 5d core level binding energies on Al(111) and Ni(111). Surf. Sci. 152/153, 272-277.

[146] Johansson B, Martensson N (1980) Core level binding energy shifts for the metallic elements. Phys. Rev. B21, 4427-4457.

[147] Tomanek D, Dowben PA, Grunze M (1983) Thermodynamic interpretation of core-level binding energies in adsorbates. Surf. Sci. 126, 112-119.

[148] Egelhoff WF (1987) Core level binding energy shift at surfaces and in solids. Surf. Sci. Repts. 6, 253-414.

[149] Frank FC, van der Merwe JH (1949) One dimensional dislocation I. Static theory. Proc. Roy. Soc. A198, 205-216.

[150] van der Merwe JH (1980) Misfit accommodation in epitaxial monolayers on (111) FCC and (100) BCC substrates. I. Analytical approach. Thin Solid Films 74, 129-151.

[151] van der Merwe JH (1982) Analytical selection of ideal epitaxial configurations and some speculations on the occurrence of epitaxy. I. Epitaxy with rectangular interfacial atomic meshes. Phil. Mag. A45, 127-143.

[152] van der Merwe JH (1982) Analytical selection of ideal epitaxial configurations and some speculations on the occurrence of epitaxy. II. Epitaxy of (111) FCC overlayers on (110) BCC substrates. Phil. Mag. A45, 145-157.

[153] van der Merwe JH (1982) Analytical selection of ideal epitaxial configurations and some speculations on the occurrence of epitaxy. III. Epitaxy of thin (111) FCC films on (110) BCC substrates by coherence. Phil. Mag. A45, 159-170.

[154] Bauer E (1958) Phänomenologische theorie jev Kristallabsheidung on oberflächen I. Z. fur Kristall. 110, 372-394.

[155] Markov I, Kaischew R (1976) Influence of the supersaturation on the mode of thin film growth. Krist. & Tech. 11, 685-697.

[156] Markov I, Kaischew R (1976) Influence of supersaturation on the mode of crystallization on crystalline substrates. Thin Solid Films 32, 163-167.

[157] Bauer E, van der Merwe JH (1987) Structure and growth of crystalline superlattices: from monolayer to superlattice. Phys. Rev. B33, 3657-3671.

[158] Richardson NV, Bradshaw AM (1984) Symmetry and electron spectroscopy. in: Electron Spectroscopy-Theory, Techniques and Applications 4, C. R. Brundle and A. D. Baker, Eds. Academic Press, New York, 153-193.

[159] Plummer EW and Eberhardt W (1982) Angle-resolved photoemission as a tool for the study of surfaces. in: Advances in Chemical Physics, I. Prigogine and S. A. Rice, Eds., Wiley, New York, 533-656.

[160] Richardson, NV (1983) Symmetry effects in the electron spectroscopy of metals with an ordered adsorbate overlayer. Surf. Sci. 126, 337-348.

[161] Hermanson J (1977) Final-state symmetry and polarization effects in angle-resolved photoemission spectroscopy. Solid State Commun. 22, 9-11.

[162] Scheffler M, Kambe K, Forstmann F (1978) Angle resolved photoemission from adsorbates; theoretical considerations of polarization effects and symmetry. Solid State Commun. 25, 93-99.

[163] Smith RJ, Anderson J, Lapeyre GJ (1976) Adsorbate orientation using angle-resolved polarization-dependent photoemission. Phys. Rev. Lett.37, 1081-1084.

[164] Smith NV, Traum MM (1973) Angular dependence of photoemission from the (110) face of GaAs. Phys. Rev. Lett. 31, 1247-1250.

[165] Smith NV, Traum MM, DiSalvo FJ (1974) Mapping energy bands in layer compounds from the angular dependence of ultraviolet photoemission. Solid State Commun. 15, 211-214.

[166] Smith NV, Traum MM (1985) Angular resolved ultraviolet photoemission spectroscopy and its application to the layer compounds TaSe2 and TaS2. Phys. Rev. B11, 2087-2108.

[167] Smith NV, Traum MM, Knapp JA, Anderson J, Lapeyre GJ (1976). Polarization effects in angle resolved photoemission using synchrotron radiation. Phys. Rev. B13, 4462-4465.

[168] Westphal D, Goldmann A (1983) Adsorbate-induced umklapp processes in photoemission from Cl on Cu. Surf. Sci. 126, 253-257.

[169] Anderson, J, Lapeyre GJ (1976) Chemisorption-induced surface umklapp proceses in angle-resolved synchrotron photoemission from W(001). Phys. Rev. Lett. 36, 376-379.

[170] Kane EO (1964) Implications of crystal momentum conservation in photoelectric emission for band structure measurement. Phys. Rev. Lett. 12, 97-98.

[171] Dowben, PA, Heskett D, Plummer EW, Sakisaka Y, Rhodin TN, Umrigar C (1984) Surface-wave-induced interference effects in angle resolved photoemission. Phys. Rev. Lett. 53, 1493-1496.

[172] Lindgren SA, Wallden L (1979) Adsorbate-induced angle averaging of Cu(111) photoemission spectra. Phys. Rev. Lett. 43, 460-463.

[173] Sakisaka Y, Rhodin TN, Dowben PA (1984) Resonant photoemission at the 3s threshold of Ni. Solid State Commun. 49, 563-565.

[174] Barth J, Kalkoffen G, Kunz C (1979) Resonance enhancement of the nickel d-band photoemission. Phys. Lett. A74A, 360-362.

[175] Iwan M, Himpsel FJ, Eastman DE (1979) Two-electron resonance at the 3p threshold of Cu and Ni. Phys. Rev. Lett. 43, 1829-1832.

[176] Clauberg R, Gudat W, Kisker E, Kuhlmann E, Rothberg, GM (1981) Nature of the resonant 6-eV satellite in Ni: photoelectron spin-polarization analysis. Phys. Rev. Lett. 47, 1314-1317.

[177] Raaen S, Murgai V (1978) Absence of two electron resonances in Valence-band spectra from Cr, Mn, Fe, and Co B36, 837-890.

[178] Kato H, Ishii T, Masuda S, Harada Y, Miyano T, Komeda T, Onchi M, Sakisaka Y (1985) Photoemission study of the existence of a valence-band satellite in Fe. Phys. Rev. B32, 1992-1996.

[179] Chandesris D, Lecante J, Petrof Y (1983) Two-electron resonances in transition metals. Phys. Rev. B27, 2630-2635.

[180] Sugawara H, Kakizaki A, Nagakura I, Ishii T (1982) Extreme ultraviolet photoelectron spectra of alpha manganese. J. Phys. F12, 2929-2936.

[181] Thuler MR, Benbow RL, Hurych Z (1982) Resonant photo- and Auger emission at the 3p threshold of Cu, Cu$_2$O, CuO. Phys. Rev. B26, 669-677.

[182] Varma S, Kime YJ, Dowben PA, Onellion M, Erskine JL (1986) Resonant photoemission at the 5p and 4f thresholds of mercury. Phys. Lett. A116, 66-70.

[183] Jansen HJF (1984) Structural properties of ferromagnetic BCC iron: a failure of the local-spin-density approximation. Phys. Rev. B30, 6177-6179.

[184] Turner AM, Erskine JL (1984) Surface electronic properties of Fe(100). Phys. Rev. B30, 6675-6688.

[185] Ohnishi S, Freeman AJ, Weinert M (1983) Surface magnetism of Fe(001). Phys. Rev. B28, 6741-6747.

[186] Turner AM, Erskine JL (1983) Magnetic exchange splitting and band dispersion of surface states on Fe(100). Phys. Rev. B28, 5628-5631.

[187] Turner AM, Donoho AW, Erskine JL (1984) Experimental bulk properties of ferromagnetic iron. Phys. Rev. B29, 2986-3000.

[188] Callaway J, Wang CS (1977) Energy bands in ferromagnetic iron. Phys. Rev. B16, 2095-2105.

[189] Peterson LG, Melander R, Spears DP, Hagstrom SBM (1976) Density of states of ferromagnetic and paramagnetic Ni and Fe studied by photoelectron spectroscopy with 21.2- and 40.8-eV photon energies. Phys. Rev. B14, 4177-4183.

[190] Scheidt H, Globl M, Dose V, Kirschner J (1983) Exchange-split empty energy band of Fe(110). Phys. Rev. Lett. 51, 1688-1691.

[191] Prutzer S, Bose SM (1985) Effects of electron-electron interaction on the valence-band photoemission spectra of metals. Phys. Rev. B31, 2762-2770.

[192] Banninger U, Busch G, Campagna M, Siegmann HC (1970) Photoelectron spin polarization and ferromagnetism of crystalline and amorphous nickel. Phys. Rev. Lett. 25, 585-587.

[193] Busch G, Campagna M, Pierce DT, Siegmann HC (1972) Photon energy dependence of spin

polarization of photoelectrons from cesiated Co. Phys. Rev. Lett. 28, 611-614.

[194] Pierce DT, Siegmann HC (1974) Hot-electron scattering length by measurement of spin polarization. Phys. Rev. B9, 4035-4037.

[195] Erskine JL, Stern EA (1973) Magneto-optic Kerr effect in Ni, Co, and Fe. Phys. Rev. Lett. 30, 1329-1332.

[196] Busch G, Campagna M, Siegmann HC (1971) Spin-polarized photoelectrons from Fe, Co, and Ni. Phys. Rev. B4, 746-750.

[197] Weller D, Alvarado SF, Campagna M, Gudat W, Sarma DD (1985) Structure, magnetism, and electronic excitations of epitaxial gadolinium (0001) on tungsten (110). J. Less-Common Metals 111, 277-283.

[198] Weller D, Alvarado SF, Gudat W, Schroder K, Campagna M (1985) Observation of surface-enhanced magnetic order and magnetic surface reconstruction on Gd(0001). Phys. Rev. Lett. 54, 1555-1558.

[199] Fernando GW, Lee YC, Montano PA, Cooper BR, Moog ER, Naik HM, Bader SD (1987) Surface electronic behavior of face-centered cubic iron on copper. J. Vac. Sci. Technol. A5, 882-886.

[200] Siegmann HC (1975) Emission of polarized electrons from magnetic materials. Phys. Rep. Phys. Lett. C17C, 37-76.

[201] Kisker E, Schroder K, Campagna M, Gudat W (1984) Temperature dependence of the exchange splitting of Fe by spin resolved photoemission spectroscopy with synchrotron radiation. Phys. Rev. Lett. 52, 2285-2288.

[202] Kisker E, Schroder K, Gudat W, Campagna M (1985) Spin-polarized angle-resolved photoemission study of the electronic structure of Fe(100) as a function of temperature. Phys. Rev. B31, 329-339.

[203] Gray LG, Hart MW, Dunning FB, Walters GK (1984) Simple compact, medium energy Mott polarization analyzer. Rev. Sci. Instru. 55, 88-91.

[204] Unguris J, Pierce DT, Galejs A, Celotta RJ (1982) Spin and energy analyzed secondary electron emission from a ferromagnet. Phys. Rev. Lett. 49, 72-76.

[205] Donohue J (1974) The Structure of the Elements, John Wiley & Sons, New York.

[206] Ross NDH, Abell JS (1970) The application of the current theories of martensite crystallography to the alpha to gamma transformation in crystalline mercury. Phys. Stat. Solidi, A1, K33-36.

[207] Weaire D (1968) On the structure of gamma-Hg. Phil. Mag. 18, 213-215.

[208] Weaire D (1968) The structures of the divalent simple metals. J. Phys. C1, 210-221.

[209] Heine V, Weaire D (1966) Structure of Di- and Trivalent metals. Phys. Rev. 152, 603-611.

[210] Worster J, March NH (1964) Electronic screening in liquids and the crystal structures of metals. Solid State Commun. 2, 245-247.

[211] Joyner RW, Roberts MW, Yates K (1979) A high-pressure electron spectrometer for surface studies. Surf. Sci. 87, 501-509.

[212] Svenson S, Martensson N, Basilier E, Malmqvist PA, Gelius U, Siegbahn K (1976) Core and valence orbitals in solid and gaseous mercury by means of ESCA. J. Electron. Spectrosc. & Relat. Phenom. 9, 51-65.

[213] Dehmer JL, Berkowitz J (1974) Partial photoionization cross sections for Hg between 600 and 250 A. Effect of spin-orbit coupling on the $^2D_{5/2}/^2D_{3/2}$ branching ratio of Hg. Phys. Rev. A10, 484-490.

[214] Becker GE, Hagstrum HD (1973) Orbital energy spectra of CO and Hg adsorbed on Ni(100). J. Vac. Sci. & Technol. 10, 31-34.

[215] Brundle CR, Roberts MW (1972) Some observations on the surface sensitivity of photoelectron spectroscopy. Proc. Roy. Soc. Lon. A331, 383-394.

[216] Egelhoff Jr WF, Perry DL, Linnett JW (1976) The adsorption of mercury on tungsten (100) studied by ultraviolet photoelectron spectroscopy. Surf. Sci. 54, 670-674.

[217] Ishi S, Ohno Y (1983) UPS from adsorbed Hg on metal surfaces. Surf. Sci. 133, L465-468.

[218] Herbst JF (1977) Angle resolved photoemission from crystal field split adatom levels. Phys. Rev. B15, 3720-3730.

[219] Himpsel FJ, Eastman DE, Koch EE, Williams AR (1980) Experimental E(k) dispersions for the Zn 3d states: Evidence for the itinerant character. Phys. Rev. B22, 4604-4609.

[220] Messervey R, Tedrow PM, Kalvey VR (1980) Proximity effect in ferromagnetic metals. Solid State Commun. 36, 969-971.

[221] Miranda R, Yndurain F, Chandesris D, Lecante J, Petroff Y (1982) Magnetic exchange splitting of a quasi two dimensional hexagonal close packed layer of cobalt. Surf. Sci. 117, 319-329.

[222] Miranda R, Yndurain F, Chandesris D, Lecante J, Petroff Y (1982) Magnetic exchange splitting of one layer of cobalt deposited on top of the (111) surface of copper. Phys. Rev. B25, 527-530.

[223] Victora RH, Falicov LM (1983) Calculation of the magnetic states of cobalt overlayers on copper (111). Phys. Rev. B28, 5232-5242.

[224] Bergmann G (1978) Transition from Pauli paramagnetism to band ferromagnetism in very thin Ni films. Phys. Rev. Lett. 41, 264-267.

[225] Moodera JS, Meservey R (1985) Detection of magnetic moments of Ni and Fe atoms on the surface of Pb. Phys. Rev. Lett. 55, 2082-2085.

[226] Kramer I, Bergmann G (1983) Magnetism of Ni poly-layers on different metallic substrates. Phys. Rev. B27, 7271-7276.

[227] Thompson MA, Erskine JL (1985) Electronic properties of p(1x1) Ni films on Cu(100). Phys. Rev. B31, 6832-6835.

[228] Huang H, Zhu X, Hermanson J (1984) Ni overlayer on a Cu(100) substrate: Magnetism and surface states. Phys. Rev. B29, 2270-2273.

[229] Wang D, Freeman AJ, Krakauer H (1982) Electronic structure and magnetism of Ni overlayers on a Cu(001) substrate. Phys. Rev. B76, 1340-1351.

[230] Gradmann U, Bergholz R (1984) Magnetization of Pd(111) films by contact with ferromagnetic Ni(111) films. Phys. Rev. Lett. 52, 771-774.

[231] Moruzzi VL, Marcus PM, Schwartz K, Mohn P (1986) Ferromagnetic phases of bcc and fcc Fe, Co, and Ni. Phys. Rev. B34, 1784-1791.

[232] Kerker GP, Ho KM, Cohen ML (1978) Mo (001) surface; a self consistent calculation of the electronic structure. Phys. Rev. Lett. 40, 1593-1596.

[233] Posternak M, Krakauer H, Freeman AJ, Koelling DD (1980) Self consistent electronic structure of surfaces: Surface states and surface resonances on W(001). Phys. Rev. B21, 5601-5612.

[234] Krakauer H, Posternak M, Freeman AJ (1979) Evidence for possible electronic contributions to the W(001) surface phase transition. Phys. Rev. Lett. 43, 1885-1889.

[235] Allan G (1978) Surface electronic structure of antiferromagnetic chromium. Surf. Sci. 74, 79-88.

[236] Allan G (1979) Condition for the existence of a permanent magnetic moment near transition metal surfaces. Phys. Rev. B19, 4774-4779.

[237] Grempel DR (1981) Surface magnetic ordering in chromium. Phys. Rev. B24, 3928-3938.

[238] Feibelman PJ, Hamann DR (1984) Quantum size effects in functions of free-standing and adsorbed thin metal films. Phys. Rev. B29, 6463-6467.

[239] Feibelman PJ, Hamann DR (1985) Surface states of clean and metal- overlayer-covered Cr(001) films. Phys. Rev. B31, 1154-1156.

[240] Gay JG, Richter R (1986) Spin anisotropy of ferromagnetic films. Phys. Rev. Lett. 56, 2728-2731.

[241] Dowben PA, Kime YJ, Varma S, Onellion M, Erskine JL (1987) Evidence for many electron effects in thin film overlayers of Hg adsorbed on Ag(100). Bull. Am. Phys. Soc. 32, 816.

[242] Kobrin PH, Heimann PA, Kerkhoff HG, Lindle DW, Truesdale CM, Ferrett TA, Becker U, Shirley DA (1983) Photoelectron measurements of the mercury 4f, 5p, and 5d subshells. Phys. Rev. A27, 3031-3039.

[243] Shannon SP, Codling K (1978) Partial photoionization cross section measurements for atomic cadmium and mercury. J. Phys. B11, 1193-1202.

[244] Shyu JS, Manson ST (1975) Angular distribution of photoelectrons from the 4f subshell of mercury. Phys. Rev. A11, 166-169.

[245] Keller F, Farnoux FC (1979) Photoionization of Hg in the soft x-ray range. J. Phys. B12, 2821-2828.

[246] Walker TEH, Waber JT (1974) Spin-orbit coupling photoionization. J. Phys. B7, 674-692.

[247] Keller F, Farnoux FC (1982) Importance of relativistic interactions in photoemission of high angular momentum electrons in mercury. J. Phys. B15, 2657-2674.

[248] Johnson WR, Radojevic V, Deshmukh P, Cheng KT (1982) Photoionization of group IIB elements. Phys. Rev. B25, 337-345.

[249] Tambe BR, Ong W, Manson ST (1981) Branching ratios of Hg 5d and Cd 4d: Dirac-Fock calculations. Phys. Rev. A23, 799-803.

[250] Johnson WR, Radojevic V (1982) Photoionization calculations for 5d, 5p, and 4f subshells of mercury. Phys. Lett. A92A 75-76.

[251] Houston JE, Peden CHF, Blair DS, Goodman DW (1986) Monolayer and multilayer growth of Cu on the Ru(001) surface. Surf. Sci. 167 427-436.

[252] Bajpai RP, Kita H, Azuma K (1976) Adsorption of water on Au and mercury on Au, Ag, Mo, and Re: Measurements of the changes in work function. Jap. J. Appl. Phys. 15, 2083-2086.

[253] Huber Jr EF (1966) The effect of mercury contamination on the work function of gold. Appl. Phys. Lett. 8, 169-171.

[254] Riviere JC (1966) The work function of gold. Appl. Phys. Lett. 8, 172.

[255] Swanson LW, Strayer RW, Davis LE (1968) Desorption, mobility, and work function change of mercury on tungsten and molybdenum substrates. Surf. Sci. 9, 165-186.

[256] Smith JR, Gay JG, Arlinghaus FJ (1980) Self consistent local-orbital method for calculating surface electronic structure: application to Cu (100). Phys. Rev. B21, 2201-2221.

[257] Smith JR, Arlinghaus FJ, Gay JB (1980) Electronic structure of silver (100). Phys. Rev. B22, 4757-4763.

[258] Shapiro AP, Wachs AL, Chiang TC (1986) Angle-resolved studies of a surface state for Ag overlayers on Cu(111). Solid State Commun. 58, 121-124.

[259] Peebles HC, Beck DD, White JM, Campbell CT (1985) Structure of Ag on Rh and its effect on the adsorption of D_2 and CO. Surf. Sci. 150 120-142.

[260] Wertheim, GK, Buchanan DNE (1986) Core-electron binding energies of adsorbed metallic monolayers: Au/Ag(111). Phys. Rev. B33, 914-918.

[261] Jaklevic RC (1984) Epitaxial growth and electronic structure of Au films on FCC(111) metals studied by electron reflection spectroscopy. Phys. Rev. B30, 5494-5499.

Editor's Note: All of the reviewer's concerns were appropriately addressed by text changes, hence there is no Discussion with Reviewers.